Quaternary International xxx (2014) 1–18

Contents lists available at ScienceDirect

Quaternary International

journal homepage: www.elsevier.com/locate/quaint

Genesis of loess-like sediments and soils at the foothills of the Banat Mountains, Romania – Examples from the Paleolithic sites Româneşti and Coşava

Holger Kels [a,*], Jens Protze [a], Valéry Sitlivy [b], Alexandra Hilgers [c], Anja Zander [c], Mircea Anghelinu [d], Manuel Bertrams [a], Frank Lehmkuhl [a]

[a] Department of Geography, RWTH Aachen University, Templergraben 55, 52056 Aachen, Germany
[b] Institute of Prehistoric Archaeology, University of Cologne, Germany
[c] Institute of Geography, University of Cologne, Germany
[d] Department of History and Letters, Faculty of Humanities, Valahia University of Târgovişte, Romania

ARTICLE INFO

Article history:
Available online xxx

Keywords:
Banat
Loess-like sediments
Albeluvisol
Fragipan
Upper Paleolithic/Aurignacian
Luminescence dating

ABSTRACT

The Paleolithic sites Româneşti and Coşava, situated at the foothills of the Banat Mountains in Romania, provide an important testament of life of the first European modern humans (*Homo sapiens sapiens*) during Middle Pleniglacial. Even though these sites have been extensively excavated, little is known about the site formation of related loess-like sediments and soils. First luminescence data at the two investigated sections confirm sediments from the penultimate glacial period to the Holocene.

Assigning the levels of findings is difficult, because the sediments are close to the surface and are overprinted by recent soil development. Albeluvisols, influenced by stagnic features, are the typical surface soils in the study area and on comparable morphological positions in the region. Laboratory analysis has revealed that this soil has a complex genesis from hydrolysis weathering, which is connected with the development of a fragic soil horizon, overprinting the major find horizons at both sites. By using sedimentological and geochemical methods in combination, this study aims to reconstruct sedimentary evolution and soil processes at the sites, as well as to evaluate the state of preservation and the actual content of the archeological contexts.

Initial results indicate hints for a forest step and higher vegetation during MIS 3 at the foothills of the Carpathian Mountains in the Western Plain of Romania. These natural factors offer a local attractiveness of the region which could be the most important reason for the occurrence of first Anatomically Modern Humans. Our investigations lend a better understanding of the paleoenvironment as well as a first age control of Paleolithic levels for the region.

1. Introduction

A new series of sedimentological and geochemical analysis, supported by luminescence dating, has focused on the investigation of loess, modern soils and paleosols at the foothills of the Banat Mountains in the western part of Romania. Unlike the more thoroughly researched, huge loess sections towards the west in Serbia (Marković et al., 2008), the occurrences of loess and loess-like sediments of the Romanian Banat have been poorly studied. Only a few studies have been published regarding sections from the Banat lowland where loess cover is more pronounced, e.g. at Semlac, Vinga and Stamora-Moraviţa (Florea et al., 1966; Conea, 1969; Conea et al., 1972). By contrast, even less is known about the genesis of thin loess-like sediments of the Banat foothills. Therefore, the new excavations of the Paleolithic sites Coşava and Româneşti (local toponym Româneşti-Dumbrăviţa) in 2009 (Sitlivy et al., 2012) offer a chance to study these archives by means of high-resolution geoarcheological investigations focused on the character of soils and sediments as well as on the state of preservation of the Upper Paleolithic find layers. A combination of granulometric and multielemental analysis supported by luminescence dating was applied to evaluate sedimentary and pedogenetic processes of these relatively thin sections embedding the archaeological levels. Typical surface soils in that region are Albeluvisols, but little is known about their complex genesis in the Banat. Questions arise about when they developed and which parent material they overprinted. What conclusions can be drawn concerning remnants

* Corresponding author.
E-mail address: holger.kels@geo.rwth-aachen.de (H. Kels).

http://dx.doi.org/10.1016/j.quaint.2014.04.063
1040-6182/

of formerly weathered horizons and the paleoclimatic impact? It is remarkable that periglacial features such as ice-wedge pseudomorphs, frost fissures, and cryoturbations are missing in the sections. However, recent studies in comparable morphological positions from the Carpathian Arc of Poland (Szymański et al., 2011) have shown that there is a wide distribution of such soil types. As these surface soils occasionally developed on Paleolithic sites, this current paper aims to elucidate the genesis of the soils and sediments in order to reconstruct the paleoenvironmental history of the region.

From the Paleolithic point of view, the Banat Paleolithic record is not particularly rich. Apart from the acknowledged Aurignacian presence, there are few traces of Middle Paleolithic, mostly the so-called Quartzitic Mousterian of the Southern Carpathians, and a single evidence of typical Mousterian with Levallois point/flake production at Gornea, as well as some Gravettian occurrences (Mogoşanu, 1978; Păunescu, 2001). The Upper Paleolithic is better known for three Aurignacian open-air sites (Fig. 1): Tincova, Coşava and Româneşti-Dumbrăviţa I and II, which had been extensively excavated during several campaigns from 1958 to 1972 (Hahn, 1970, 1977; Mogoşanu, 1978; Băltean, 2011). The single-layered workshop at Tincova contains abundant waste products and only 110 formal tools. The toolkit is dominated by endscrapers with a few carinated, nosed, nucléiformes, rabots, many Dufour bladelets, and several Font-Yves points (Mogoşanu, 1978). During the recent debates on the definition of the Aurignacian, some scholars have considered Tincova to be a good candidate for inclusion in the Protoaurignacian phenomenon (Zilhão, 2006, Teyssandier, 2007, 2008; Zilhão et al., 2007), but Coşava and Româneşti still need to be discussed. Apart from technological discussions by prehistorians, little is known about the site formation processes. Thus, the main objective of this current study is to investigate in detail the paleoenvironmental and paleoclimatic context of the first anatomically modern humans (*Homo sapiens sapiens*) in Europe during Marine Isotope Stage (MIS) 3.

2. Study area

The Banat foothills are located in the eastern part of the historical region of Romanian Banat, in the transition zone from the Carpathian Mountains to the eastern branch of the Pannonian Basin (Fig. 1). In this region, Neogene silts and sands are exposed close to the surface. Beneath that is the geomorphologic setting dominated by hilly piedmont plains and local terrace steps (Posea, 1975). In some places, the uppermost part is covered by a thin layer of loess and loess-like sediments.

The sites of Coşava I (45°51′11.92″ N, 22°19′32.71″ E) and Româneşti I (45°49′02.41″ N, 22°19′15.12″ E) are situated in the catchment of the upper Bega River system (Fig. 1). The Bega River is a tributary of the Timiş River and represents one of the most important drainage systems from the Carpathian Mountains and the Western

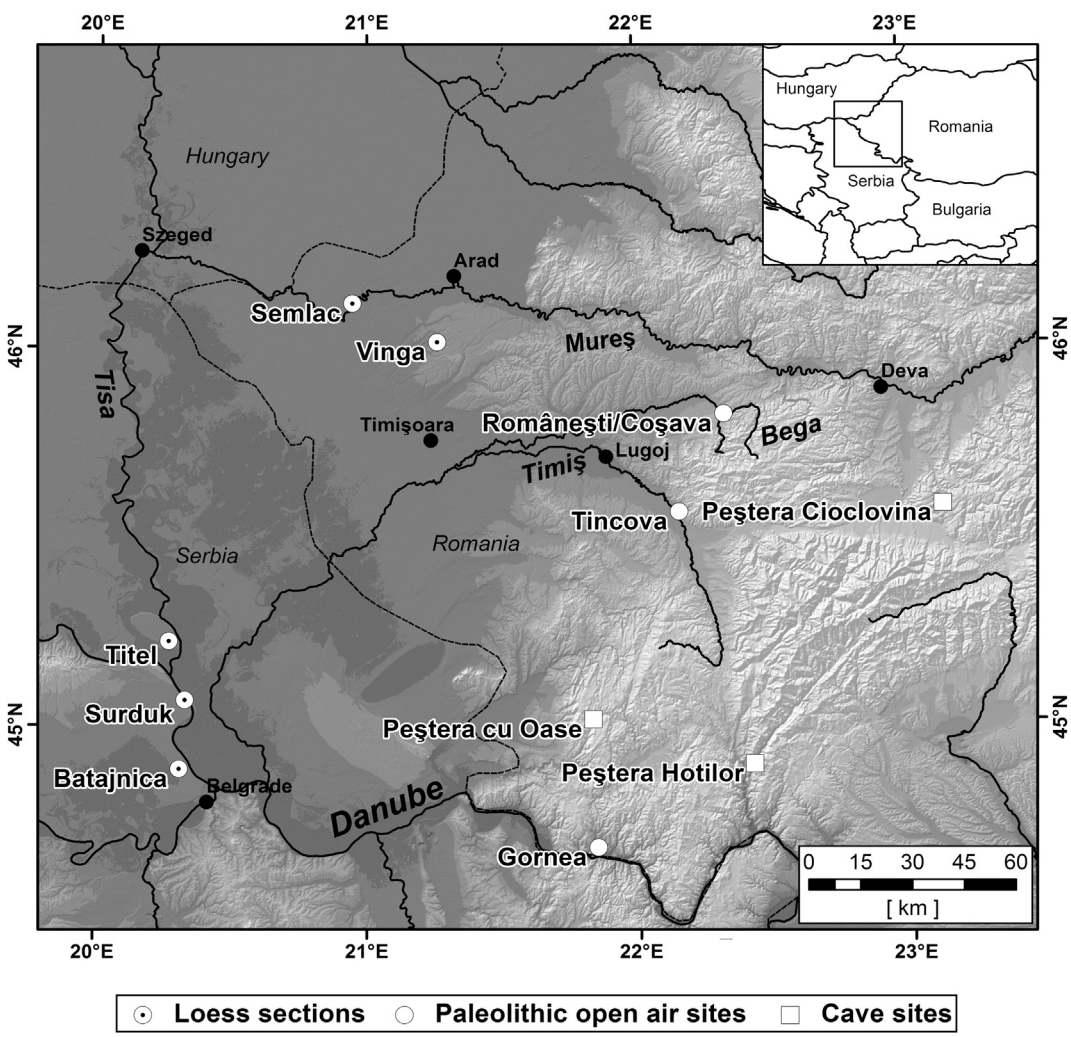

Fig. 1. Romanian Banat: Regional setting, positions of selected loess sections, Paleolithic open air sites and cave sites (Projection: UTM 34 WGS 1984, Source of SRTM data: Jarvis et al., 2008; Cartography by R. Löhrer).

Please cite this article in press as: Kels, H., et al., Genesis of loess-like sediments and soils at the foothills of the Banat Mountains, Romania – Examples from the Paleolithic sites Româneşti and Coşava, Quaternary International (2014), http://dx.doi.org/10.1016/j.quaint.2014.04.063

Plain. The Bega River system originates in the Poiana Ruscă Mountains, about 15 km to the south and southeast of the Româneşti site.

The study area has moderate continental climate with a mean annual precipitation of 600–800 mm and mean annual temperatures of 9–10 °C (Mavrocordat, 1971; Gâstescu et al., 1975). In comparison to the drier lowland in the west (annual precipitation: 500–600 mm, mean temperature: 10–11 °C), these climatic conditions lead to a different vegetation cover and soil development. Consequently, Luvisols and Albeluvisols are the dominant soil types in the Carpathian foothills (Ianoş, 2002). Albeluvisols show a strong soil development often affected by redoximorphic influences resulting in the formation of a Stagnic Albeluvisol (German: "Pseudogley-Fahlerde", AG Boden (2005), Romanian: "sol (podzolic) argilo-iluvial pseudogleizat" (Mavrocordat, 1971). In the Romanian System of Soil Taxonomy (RSST-2000), Albeluvisols belong to the genetic soil type "Luvosol" (Munteanu and Florea, 2001) which develops in morphological positions where precipitated water percolates in more slowly, thereby trapping moisture and resulting in the formation of intense stagnic features.

The most obvious feature of Albeluvisols is their subdivision in three general horizons (Driessen et al., 2001; IUSS Working Group WRB, 2007). The lowermost argillic horizon is rich in brownish to reddish clay and overlain by a leached horizon, poor in clay and iron oxides caused by outwash effects. From this horizon, tongues of bleached sediment penetrate into the argillic horizon and form an irregular top of the latter. In general, the albeluvic tongues can be related to desiccation cracks, ice-wedge pseudomorphs or fossil root channels. However, as polygonal structures were not discerned in the planum at both sites, the bleached tongues are most likely associated to former root channels. Finally, a humic horizon makes up the uppermost layer of the Albeluvisols.

2.1. Coşava site

The site of Coşava (Figs. 1 and 2) is situated on a plateau spur east of the village at an altitude of up to 282 m above sea level (asl) and more than 90 m above the level of the Bega River. On this plateau, sandy loess-like sediments with a thickness of up to 1.5 m cover light grayish-white silty sands originating from the Tertiary. The main slope is deforested and dominated by grass, serving as grazing ground for sheep and goats.

Previous excavations at Coşava (Mogoşanu, 1978) have yielded three Upper Paleolithic layers, at least the two lowermost of which comprise Aurignacian tools without admixture. The most representative layer (I) contains 110 tools. Contrary to the Tincova site (Fig. 1), the toolkit is dominated by carinated and nosed endscrapers, associated with abundant retouched blades, including Aurignacian blades, several dihedral burins, a single Dufour bladelet and one Font-Yves point. Layer II comprises 56 tools with a comparable typological composition. The uppermost layer III (24 tools) contains Aurignacian types (5 Dufour, 2 carinates and one Font-Yves point) as well as some Epi-Paleolithic elements (Mogoşanu, 1978).

Cos 1 (Fig. 3, Table 1; Coşava I, trench 2, profile E, square 286/509–286/507) is one of the main sections of re-excavation at Coşava with typical strata and horizons of the upper plateau spur. Single well-rounded pebbles, dominated by quartz, lydite, quartzite and different metamorphic stones, appear as a thin gravel layer all over the plateau in the deeper part of the thin and sandy-to-silty sediment cover, exposed on the hill slopes to the southeast. A thicker, laminated package of gravel with finer components, sands and typical features of an *in situ* terrace-sediment or a package of gravel from piedmonts is missing on this plateau spur. At different positions, it seems as if underneath the level of the pebbles, remnants of a reddish-brown fossil horizon with weak reddish clay coatings on the texture were preserved. From the intensity of this horizon, we initially inferred interglacial soil development, which may be demonstrated by laboratory analysis in this study. Above the thin gravel layer, the sandy but siltier sediment overlies the gravel, with thicknesses of up to one meter. The soil development in this layer begins with a dense argillic horizon, characterized by an accumulation of iron (Fe) and manganese (Mn) nodules in the lower half. Up to four levels of fossil root channels have been detected within the argillic horizon, but relicts of overprinted weak A- or B-horizons from where they originated cannot be detected in the field due to strong overprinting of the stagnic Albeluvisol. The fillings of these root channels are bleached; some show humic-brownish color. If they were connected to former surfaces, soil development and sedimentation proceeded.

Table 1
Field description of Coşava I, Profile 1 (see also Fig. 3).

Unit	Depth of base b.s. (cm)	Pedogenic horizon		Texture	Description
		After FAO	After KA 5		
III	4	O	O	U, u, s	Dark-grayish brown, crumb structure, intensively rooted (grass), few single fine pebbles
	18	Ah	Ah	U, u, s	Dark-grayish brown, crumb structure to platy subangular block structure, humic, intensively rooted (grass), weakly spotted with rust (<1 mm), worm castings, biogalleries at the base, few single fine to medium gravel
	25	E	AE	U, u	Light grayish-brown, weakly bleached, weak subangular blocky structure, weakly rooted (grass), spotted with rust and manganese (<1 mm), worm castings, few single fine to medium gravel
	45	M	M	U, u	Light brownish, subangular blocky structure, spotted with rust and manganese (<1 mm–2 mm), reworked sediment (colluvial), worm castings, fine rootlets (grass), few single fine gravel
	(55–85)	(E)	(E)	U, l, s	Light brownish, weak subangular blocky structure, spotted with rust, bleached root channels and cracks towards the underlying horizons (rusty edged in the lower part) [As the originated bleached horizon was eroded by the overlying horizon, we took bulk samples from the bleached tongues]
II	70	EBtx	EBtx	U, l	Brown, subangular blocky structure, argillic, spotted with rust and manganese (<1 mm–1 cm), bleached and rusty edged root channels of the overlying horizon (light grayish) and smaller root channels within the horizon (fossil, more grayish)
	105	2Btx	Btx1	U, l, s	Reddish-dark brown, subangular blocky structure, argillic, intensively spotted with rust and manganese (1 mm–2 cm), bleached and rusty edged root channels of the overlying horizon (light grayish) and smaller root channels within the horizon (fossil, more grayish), few single fine to medium gravel
	118	3Btx	Btx2	U, l, s	Reddish-brown, angular blocky structure, argillic, intensively spotted with rust and manganese (1 mm–1 cm), few clay coatings, few root channels within the horizon (fossil, more grayish) few single fine to medium gravel
I	150*	BC	BC	U, s	Brownish gray, subangular blocky structure, weakly spotted with rust and intensively spotted with manganese (2 mm–2 cm), weakly gleyic, few root channels within the horizon (fossil, more grayish)

b.s. = below surface/* = Base of lowermost horizon not excavated/designation of soil horizons after FAO (FAO, 2006) and KA 5 (AG Boden, 2005)/C = clay, U = silt, l = loamy, s = sandy, u = silty.

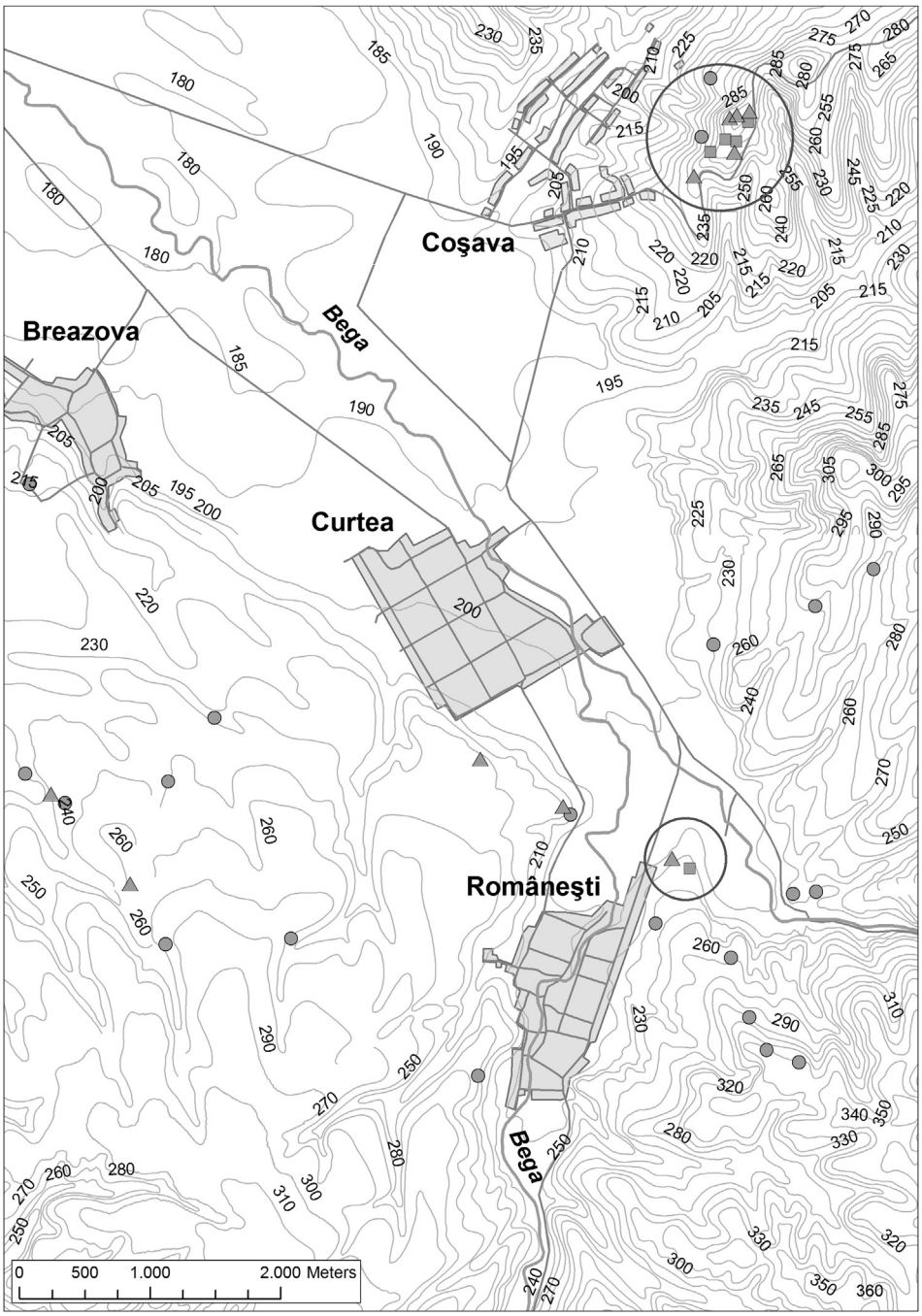

Fig. 2. The Paleolithic sites Româneşti and Coşava and further surveyed places in the upper Bega catchment (circles = Paleolithic sites, dots = prospected positions without findings, triangles = prospected positions with Paleolithic artefact occurrences).

Bleached tongues penetrate into the argillic zone. A bleached horizon above this zone is missing because of erosion, as manifested by a light brownish colluvial layer on top. Above this layer and below the humic horizon, a very weak light brown horizon (potentially bleached) can be distinguished. Paleolithic artifacts have been located above the pebble-layer at a depth of 15–80 cm. Analogous to Mogoşanu (1972, 1978), we distinguished three separate layers of findings with Paleolithic assemblages (levels GH 4, 3, and 1 to 2 in Fig. 3; see Sitlivy et al., in this volume). Upon a first macroscopic consideration, the argillic horizon above the pebbles could not be subdivided pedologically in most of the sections on the plateau.

2.2. Româneşti site

The Paleolithic site of Româneşti I is located at a lower topographic position 4 km south of Coşava (Figs. 1 and 2). The altitude of this site is around 212 m asl, much lower than the Coşava site and around 10 m above the level of the Bega River close to the confluence of the rivers Bega Mică and Bega Mare. The land use is characterized by meadows with some plum trees and ploughed fields. The reference profile of the first investigation site (Rom 1, Fig. 4, Table 2) was developed in a flat position on a terrace step.

Please cite this article in press as: Kels, H., et al., Genesis of loess-like sediments and soils at the foothills of the Banat Mountains, Romania – Examples from the Paleolithic sites Româneşti and Coşava, Quaternary International (2014), http://dx.doi.org/10.1016/j.quaint.2014.04.063

Table 2
Field description of Românești I, Profile 1 (see also Fig. 4).

Unit	Depth of base b.s.(cm)	Pedogenic horizon		Texture	Description
		After FAO	After KA 5		
III	4	O	O	U, l	Brown, crumb structure, intensively rooted (grass), few single fine pebbles
	15	Ap	Ap	U, l	Brown, crumb structure, rooted (grass), weakly spotted with rust, few single fine to medium gravel
	25	M	M	U, l	Grayish-brown, subangular blocky structure, weakly spotted with rust and manganese (<1–4 mm), few single fine to medium gravel, pieces of pottery, colluvic material
	34	Bw	Bv	U, l	Light grayish-brown, subangular blocky structure, weakly spotted with rust and manganese (<1–4 mm), silex artifact
	45	E	E	U, l	Grayish-light brown, bleached, subangular block structure, spotted with rust and manganese (<1–10 mm), bleached root channels and cracks towards the underlying horizons
II	60	EBtx	EBtx	U, l	Reddish-light grayish brown, angular blocky structure, argillic, intensively spotted with rust and manganese, bleached and rusty edged root channels of the overlying horizon (light grayish) and smaller root channels within the horizon (fossil, more grayish), silex artifacts
	90	2Btx	Btx	U, l	Reddish-light grayish brown, angular blocky structure, argillic, intensively spotted with rust and manganese, manganese concretions (>1 cm), some fossil root channels
I	130	Bg	Gro	C, u	Brownish-light bluish-gray, weak prismatic structure, spotted with rust

b.s. = below surface/* = Base of lowermost horizon not excavated/designation of soil horizons after FAO (FAO, 2006) and KA 5 (AG Boden, 2005)/C = clay, U = silt, l = loamy, u = silty.

Through test drilling, the top of a thicker package of gravel could be verified 2.80 m below the surface. This gravel had been mentioned by Mogoşanu (1978). As observed in a sunken road nearby the village, this gravel covers a thickness of more than 2 m, potentially representing a former terrace of unknown age. The gravel is covered by sandy to increasingly silty, loess-like sediments towards the top at the section Rom 1. As tested by drilling, no gravel layer can be found within the silt cover for the uppermost 2.80 m.

Mogoşanu (1978) defined six layers of findings at Românești-Dumbrăviţa I: the Aurignacian layers (II, III, IV, and V) were recorded between a quartz flake industry apparently belonging to the Mousterian and a thin Gravettian layer. The richest assemblage (>5000 items, including 114 tools) was recovered from layer III and comprised endscrapers (including carinated ones), fewer burins, 8 Dufour bladelets and several retouched blades. Layer IV differed from the previous one by the presence of truncated blades/flakes, several endscrapers, and a larger number of burins. Aurignacian-type forms appeared less common and Dufour bladelets were absent. Layer V contained an assemblage rich in debitage products, with a few tools, mostly burins. Aurignacian-type forms appeared less common in this layer. In contrast to Mogoşanu's observations, we distinguished four separate layers of findings with Paleolithic

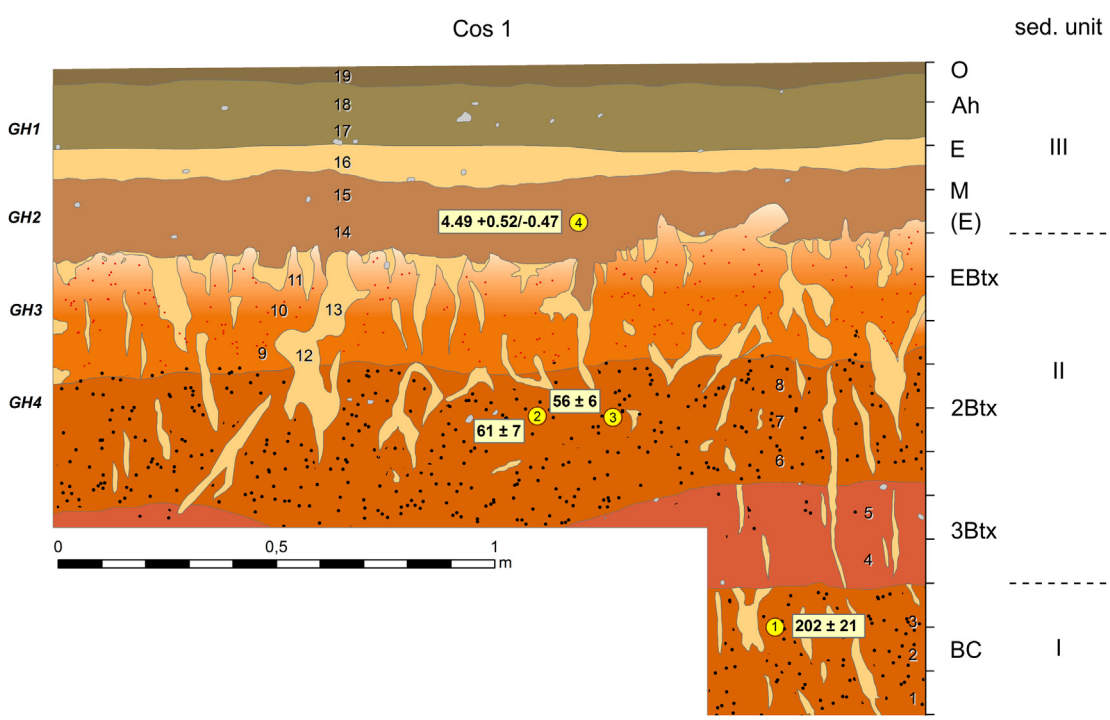

Fig. 3. Cosava I, Profile 1, Trench 2, eastern section. Labelling of samplings for sedimentology and geochemistry, positions of samples for luminescence and luminescence ages, see Table 4 for more details (1 = COS1-1, 2 = COS1-2a, 3 = COS1-2b, 4 = COS1-3), GH = compiled layers of findings from the excavation in 2009.

Please cite this article in press as: Kels, H., et al., Genesis of loess-like sediments and soils at the foothills of the Banat Mountains, Romania – Examples from the Paleolithic sites Românești and Coşava, Quaternary International (2014), http://dx.doi.org/10.1016/j.quaint.2014.04.063

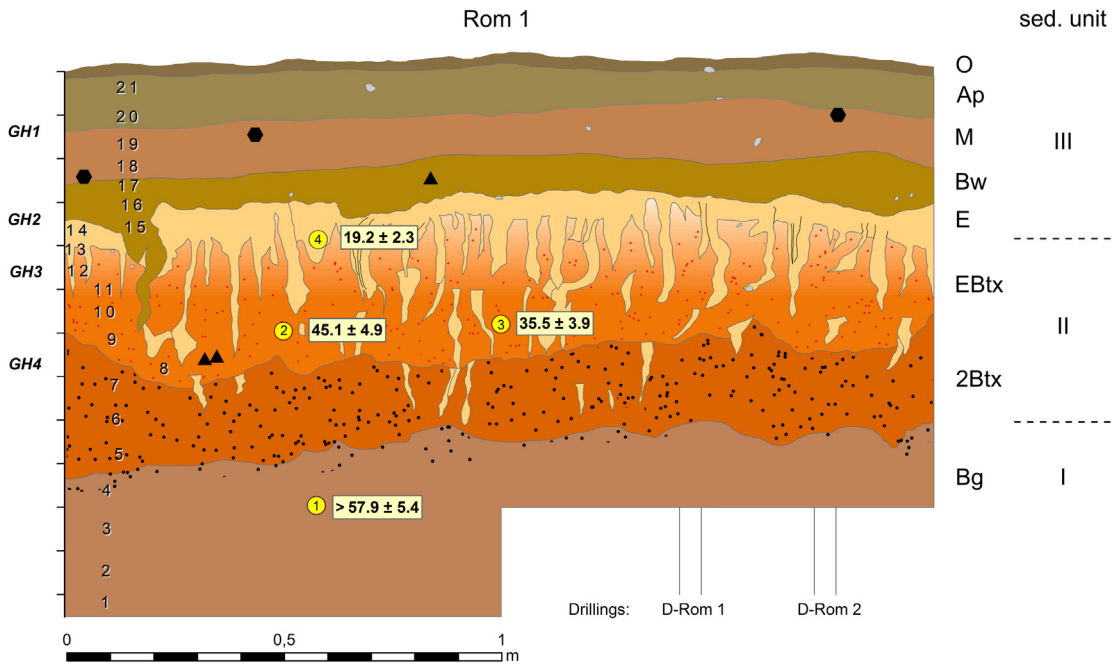

Fig. 4. Romanesti I, Profile 1, eastern section: labelling of samplings for sedimentology and geochemistry, positions of samples for luminescence and luminescence ages, see Table 4 for more details (1 = ROM1-3, 2 = ROM 1-4a, 3 = ROM 1–4b, 4 = ROM 1–5), GH = compiled layers of findings from the excavation in 2009, findings from the profile: black triangles = lithics, pentagon = pottery.

artifacts (levels GH 4 to 1 in Fig. 4; see Sitlivy et al., 2012), whereas the main concentration of the Aurignacian lithic assemblage belongs to GH 3.

Compared to the Coşava site (Fig. 3, Table 1), the morphological position and the geological composition of the sediments and soils differ at Româneşti. The sedimentary sequence is generally finer. The lowermost part of the section is rich in clay and was formerly affected by groundwater. As in Coşava, the surface soil above is a type of stagnic Albeluvisol. However, field observations have found that the dense argillic horizon does not show such intense clay coatings on the texture as was detected in the lower part of Coşava section. At both sections, this horizon is rather tough to excavate and displays cemented features.

In Rom 1, we found up to four levels of fossil root channels within the argillic horizon, but as in Coşava, there is no evidence for relicts of overprinted weak A- or B-horizons. At the Româneşti section, the accumulation of Fe- and Mn-nodules in the lower half of the argillic horizon is more intensive and, here, a bleached horizon overlies. Underneath the ploughed horizon and above the bleached horizon, there is a thin colluvial layer that includes pottery of Neolithic to Medieval age.

3. Archeological background: results from the re-excavation of the Paleolithic sites Coşava and Româneşti

The Banat Aurignacian sites had remained undated before this current study. Based on pollen analysis (Mogoşanu, 1978; Cârciumaru, 1989, 1978), the initial geochronological estimations appeared surprisingly late: Herculane/Tursac (Tincova) and Herculane II/Laugerie (level III in Româneşti), despite the content of the lithic collections, pointing to an older Aurignacian stage (Chirica, 1996). The initial excavator, Fl. Mogoşanu, had noted the similarities between Tincova, Coşava (level I), Româneşti-Dumbrăviţa I (level III), and Krems-Hundssteig in Austria. Due to the late geochronological assessments, however, he concluded that the Banat settlements represented a "late echo" of this Central European Aurignacian variant. According to more recent reassessments (Teyssandier, 2003; Zilhão, 2006), the Tincova assemblage nonetheless seems to be rather comparable to the Proto-aurignacian, generally dated around 37 ka uncal BP and, thus, predating the Early Aurignacian in Europe (ca. 35 uncal ka BP). As the reframing of Tincova ignored the similitudes initially recorded between the three Banat settlements and also lacked a direct chronological support, the need for new archeological and geochronological investigations appeared obvious (Anghelinu and Niţă, in this volume; Anghelinu et al., 2012).

The recent re-examination of the old collections from Coşava I and Româneşti I generally confirms Mogoşanu's initial conclusions. However, the results of the new excavations in both sites led to strikingly different general artifact/tool densities and/or lithic compositions (e.g. prevalence of "micro-artifacts") when compared to previous research. For instance, a test pit at Româneşti I in 2009 yielded over one thousand artifacts in an area of 1 m^2 by means of wet sieving, whereas the old published collection accounts 5278 artifacts recovered from a total excavated area of 450 m^2. The same is true for Coşava (2009), where a few test pits yielded more retouched Dufour bladelets and chips than the old, extensive excavations.

The lithic assemblages recovered from Coşava I during the first field campaign are quite modest (for details, see Sitlivy et al., in this volume). Test pits have delivered a total of 413 lithics, originating from all three of Mogoşanu's layers, namely from the base to the top: layer I/geological horizon 4 (hereafter GH, where this term is used to describe general units during excavation) (91 artifacts), layer II/GH 3 (127 artifacts) and layer III/GH 1-2 (195 artifacts). The Româneşti I lithic sample from 2009 to 2010 amounts to 7505 lithic artifacts, mostly recovered from GH 3. Although Coşava's sequence displays remnants of three archeological layers which can be tentatively correlated to the old data, the situation looks different in Româneşti, where the small size of the new excavations could neither confirm nor reject the existence of six Paleolithic layers as defined by Mogoşanu (1978). The newly excavated Aurignacian assemblage here appears sandwiched between a likely Middle Paleolithic layer

Please cite this article in press as: Kels, H., et al., Genesis of loess-like sediments and soils at the foothills of the Banat Mountains, Romania – Examples from the Paleolithic sites Româneşti and Coşava, Quaternary International (2014), http://dx.doi.org/10.1016/j.quaint.2014.04.063

with isolated quartz artifacts and a Gravettian one, with the lowermost layer I at the bottom (GH 4) and the Gravettian layer VI at the top (GH 1 and 2). Although the vertical artifact density varies, the Aurignacian-looking inventory is not sterile and occurs continuously throughout the upper part of GH 4 and the whole of GH 3. Moreover, judging from artifact labels from the old collection, a similarly continuous vertical distribution of finds can be inferred. Given the fact that the former layer separation was mainly based on horizontal clusters, it thus remains hard to define the precise number of different occupations preserved by the short sequence here (for details, see Sitlivy et al., in this volume; Sitlivy et al. 2012).

The observations made on the Aurignacian toolkits from both sites, much like the reappraisal of the old collections, generally converge in supporting the rather "archaic/early" technological character of the corresponding archeological layers. Worth noting is the variability of bladelet production, based on reduction of different carinated pieces, prismatic cores and core-on-flakes, followed by blank modification through fine semi-abrupt retouch into Dufour sub-type bladelets or Font-Yves/Krems points. However, the assemblages' composition varies considerably in terms of "micro/macro" artifacts/tools, especially when compared to the old collections. Several factors (e.g., different excavated surfaces and recovering methods, diverse artifact clustering) can explain the contrast. Moreover, the "early" technological and typological Aurignacian characteristics should be supported by the dating record and multidisciplinary studies, taking into consideration that the "archaic" features alone cannot sustain any precise chronological scenario.

4. Methods

4.1. Sedimentological and geochemical analysis

Designation of sediments and soil horizons and classifications of textural classes are given using FAO (FAO, 2006; IUSS Working Group WRB, 2007) and AG Boden (2005). Soil samples from the sections were taken at 5–10 cm intervals for sedimentological and geochemical analysis.

In the laboratory, all samples were air dried, homogenized, and sieved to <2 mm. Iron–manganese concretions with a grain size larger than that of coarse sand were removed. For particle-size analysis, the samples were air-dried. As the sections were already decalcified, it was not necessary to dissolve the carbonates by HCl. To remove the organic matter, the samples were treated with 0.70 ml 20% H_2O_2 at 70 °C for several hours. This process was repeated four times over a period of two days. To keep particles dispersed, the samples were treated with 1.25 ml, 0.1 M sodium-pyrophosphate ($Na_4P_2O_7 \times 10H_2O$) for 12 h (Pye and Blott, 2004). Particle size was measured with a Laser Diffraction Particle Size Analyzer (Beckman Coulter LS 13 320) by calculating the mean diameters of the particles within a size range of 0.04–2000 μm with an error of 2%. Each sample was measured four times in two different concentrations to increase accuracy. Afterwards, all measurements with reliable obscuration were averaged. To avoid the problem of underestimation of the clay fraction relative to the silt fraction by using the Fraunhofer optical theory for the laser diffraction particle size analysis (Eshel et al., 2004), the Mie-theory was applied as additional optical model for the silt and clay fractions and different shape factors (Sf) for correction of the spherical characteristics of the particles (as proposed by ISO 13320 (2009)). For the Mie theory, a refractive index (RI = 1.55) and an absorption index (AC = 0.1) was used as proposed by Özer et al. (2010).

In addition to the conventional laser diffraction following the ISO 13320 (2009), the differences between both optical models (Fraunhofer–Mie) were calculated to obtain further information on grain shape and crystallinity. The difference was determined for the fractions clay and fine sand, as these grain size classes are further away from each other. With respect to the fine sand fraction, it has to be considered that the difference between the two optical models is at 0 ± 0.2%. The higher the negative variation, the more transparent the particles of a fraction are. For terrestrial archives, this is valid for quartz (SiO_2). Based on the Fraunhofer model, grain-size measurements are less exact, because this optical model does not consider the refraction of the laser through the particle. If the variety for fine sand is higher than 0.2, there could be a mineral or material change within the sample. In this case, higher contents of mica, feldspar, and pyroxene can be suggested. The relative underestimation of the Mie theory model for this range can be explained by a varying refraction and absorption of the laser. The latter is valid for samples with higher amounts of manganese or carbon that resulted in a "darkening" of the samples. Therefore, the imaginary adsorption index of 0.1 (Özer et al., 2010) is not useful; instead, it is recommended to use the adsorption index of 0.2 (Buurman et al., 1997). To keep the comparability, we used the Mie theory model based on Özer et al. (2010) for this study. Within the clay fraction, the difference between the optical models is always negative. A larger difference implies a more spherical particle, and the lower value indicates a flat particle structure. The particle size scales are defined by using ISO 14688 (2002), where clay (Cl) < 2 μm, fine silt (FSi) = 2–6.3 μm, medium silt (MSi) = 6.3–20 μm, coarse silt (CSi) = 20–63 μm, fine sand (FSa) = 63–200 μm, and medium sand (MSa) = 200–630 μm (Blott and Pye, 2012).

The determination of elements ranging from sodium (Na, $n = 11$) to uranium (U, $n = 92$) was conducted by polarization energy dispersive X-ray fluorescence (EDPXRF) using a Spectro Xepos. The bulk sediment samples were screened down to 63 μm and dried at 105 °C for 12 h. All samples were prepared as pressed (30 t) to powder pellets, and measurements were conducted by means of a pre-calibrated method (38 KeV, 10 W). The data correction followed the fundamental parameter method. All samples were measured twice; for statistical analyses, the arithmetic mean was applied.

Soil color measurements based on the CIE $L^*a^*b^*$ color system (Commission Internationale de l'Eclairage, 1978) were applied on dried and homogenized soil samples (sieved to <2 mm) with a Chroma Meter CR-400/410 (Konica Minolta). The CIE $L^*a^*b^*$ system expresses the extinction of light as luminance on a scale from L^* 0 (absolute black) to L^* 100 (absolute white), and color as chromaticity coordinates on red–green (a^*) and blue–yellow (b^*) scales. Based on the b^* color value, the iron fractions were determined (Scheinost, 1995; Scheinost and Schwertmann, 1999). pH-value was measured in a 0.01 M $CaCl_2$-suspension by using a pH-Meter (Knick pH-Meter 766 Calimatic).

4.2. Luminescence dating

Four samples from Coşava (section Cos 1, Fig. 3) and four samples from Româneşti (section Rom 1, Fig. 4) were dated by luminescence at the laboratory of the Institute of Geography in Cologne to provide information on the geochronological context. For luminescence dating, two parameters have to be determined: the dose rate (D_0, in Gy/ka) and the equivalent dose (De in Gy). The annual dose rate derives from the decay of lithogenic radionuclides such as uranium, thorium, and potassium in the sediment. The concentration of these elements was measured by high-resolution gamma ray spectrometry (Table 3). Attenuation of ionizing radiation is more effective in sediments with water-filled interstices. As the actual water contents of the samples, which were determined by weight loss after drying (see Table 3), are not fully representative for the changes in sediment moisture over the entire period of burial, water content variations of 17 ± 5% (Coşava) and 20 ± 5% (Româneşti) were finally assumed for age calculation.

Table 3
Results of the gamma-ray spectrometry and further parameters relevant for dose rate calculation. All values are shown with their 1 sigma-error.

Lab. Code	Sample ID	Water content (measured, weight-%)	Depth (m)	U (ppm)	Th (ppm)	K (%)
C-L2686	COS1-1	17.9	1.28	2.13 ± 0.11	8.77 ± 0.51	0.84 ± 0.03
C-L2687	COS1-2a	7.7	0.80	2.52 ± 0.11	10.62 ± 0.55	1.03 ± 0.03
C-L2688	COS1-2b	9.4	0.80	2.54 ± 0.11	10.42 ± 0.55	1.03 ± 0.03
C-L2689	COS1-3	16.6	0.36	2.31 ± 0.12	8.68 ± 0.50	0.91 ± 0.04
C-L2694	ROM1-3	23.5	1.03	3.39 ± 0.15	13.85 ± 0.72	1.33 ± 0.04
C-L2695	ROM1-4a	16.5	0.60	3.81 ± 0.16	13.95 ± 0.72	1.27 ± 0.04
C-L2696	ROM1-4b	14.9	0.57	3.50 ± 0.15	14.39 ± 0.75	1.28 ± 0.04
C-L2697	ROM1-5	15.1	0.40	3.81 ± 0.16	14.05 ± 0.73	1.42 ± 0.04

For luminescence dating, the sand-sized quartz and the K-rich feldspar fractions were extracted from bulk sediments (see Table 4 for the grain sizes used for dating). The samples were prepared analogously to those procedures reported by Hilgers et al. (2001). Typically, finer grain sizes (e.g. 4–11 μm) are used for dating loess deposits. Because reworking of the sediments could not be excluded at the sites investigated in this study, we have chosen larger grain sizes to enable analysis of small sub-samples (aliquots) containing only a few tens to hundreds of grains instead of several thousands. Reducing the grain number per aliquot improves investigation of the dose variability potentially caused by insufficient signal re-setting during transport and deposition (Duller, 2008). In order to obtain a reliable equivalent dose estimate, several sub-samples or aliquots, respectively, were measured for each sample (see Table 4 for more experimental details regarding the luminescence measurements). Each aliquot consists of multiple mineral grains, in this study roughly about 80 up to a few hundred grains on average, depending on the grain size used for dating (Table 4). Galbraith et al. (1999) described several methods to combine individual De values of a sample to obtain the appropriate average equivalent dose to be used in the age calculation. Here, the choice of model was based on the shape of the De distribution, which was assessed visually from radial plots (Galbraith, 1988; see Fig. S1), and on the overdispersion value, which describes the relative spread in equivalent doses remaining after taking measurement uncertainties into account. For all samples, irrespective of the applied protocol or mineral used for luminescence measurements, the observed data spread was larger than could be explained by the individual error of each analysis (all OD-values >0, Table 4). Hence, in a first attempt the average De value was calculated following the 'central age model' (CAM) that is appropriate for overdispersed De distributions (Galbraith et al., 1999). The CAM assumes that all grains received similar doses, centered on an average De, but were still deposited in the same depositional event. Thus, on a 2-sigma level, the individual De values would agree with the central dose value. This was observed for most of the feldspar measurements. Several samples showed a substantial data spread most probably caused either by post-sedimentary intrusion of younger material through root channels or desiccation cracks or older material through bioturbation or by insufficient re-setting of the luminescence signals at the time of burial (see Fig. S1). For these samples, the minimum age model (MAM, Galbraith et al., 1999) or the median was used for calculating the average equivalent dose of those sub-samples considered to be the best representative for the 'true' burial dose or for the majority of sub-samples, respectively (Table 4, Fig. S1).

Table 4
Results of equivalent dose (De) measurements, dose rate and age calculation. All values are shown with their 1-sigma-error. The dose rates include the cosmic dose contribution which was calculated according to the present sampling depth (Prescott and Hutton, 1994) and are calculated for an assumed average water content of 20 ± 5% (for sample series ROM1) and 17 ± 5% (for sample series COS1). A 5% uncertainty for the beta source calibration was incorporated in age calculation. The most reliable age estimates are shown in bold print. Ages estimates printed in italics are considered to underestimate the true depositional age due to fading and should be interpreted as minimum ages only. For the pIRIR approach applied to K-rich feldspars uncorrected ages are presented as well as ages obtained after subtraction of a dose residual of 16.84 Gy was determined after bleaching for 1 h in a solar simulator. Note that $IRSL_{50}$ ages do not refer to the IR_{50}-signal obtained during the pIRIR-measurement cycles, but to individual measurements using the SAR-$IRSL_{50}$ protocol. (Q = quartz, KF= Potassium-rich feldspars).

Lab. Code	Sample ID	Measured mineral, grain size, and protocol[a]	Age model[b]	De (Gy)	n[c]	OD (%)[d]	Dose rate (Gy/ka)	Luminescence age (ka)
C-L2686	COS1-1	KF, 100–200 μm, $IRSL_{50}$	CAM	369 ± 14	10	11.1	2.43 ± 0.18	*152 ± 15*
		KF, 100–200 μm, $pIRIR_{290}$	CAM	506 ± 28	9	13.6	2.43 ± 0.18	209 ± 22
								202 ± 21 (residual subtracted)
C-L2687	COS1-2a	KF, 100–200 μm, $IRSL_{50}$	CAM	157 ± 11	15	25.8	2.80 ± 0.20	*56 ± 6*
C-L2688	COS1-2b	KF, 63–200 μm, $IRSL_{50}$	CAM	195 ± 7	12	12.1	2.77 ± 0.21	*70 ± 7*
		KF, 100–200 μm, $pIRIR_{290}$	Median	187 ± 14	8	18.3	2.79 ± 0.20	67 ± 8
								61 ± 7 (residual subtracted)
C-L2689	COS1-3	Q, 100–200 μm, OSL	MAM	8.67 +0.56/−0.38	65	38	1.93 ± 0.16	4.49 +0.52/−0.47
C-L2694	ROM1-3	KF,100–200 μm, $IRSL_{50}$	CAM	194 ± 7	10	9.8	3.35 ± 0.24	*> 57.9 ± 5.4*
		KF, 63–100 μm, $pIRIR_{290}$	Unreliable, close to saturation					
C-L2695	ROM1-4a	Q, 100–200 μm, ITL_{310}	CAM	128 ± 5	19	16.3	2.76 ± 0.21	46.6 ± 4.6
		KF, 63–100 μm, $pIRIR_{290}$	Median	166 ± 9	12	22.7	3.31 ± 0.27	50.2 ± 5.4
								45.1 ± 4.9 (residual subtracted)
C-L2696	ROM1-4b	KF, 100–200 μm, $IRSL_{50}$	CAM	90.2 ± 5.0	11	14.7	3.38 ± 0.24	*26.7 ± 2.8*
								29.7 ± 5.5 (fad. corr.)
		KF, 63–100 μm, $pIRIR_{290}$	CAM	133 ± 8	11	18.2	3.28 ± 0.26	40.6 ± 4.5
								35.5 ± 3.9 (residual subtracted)
C-L2697	ROM1-5	KF, 100–200 μm, $IRSL_{50}$	CAM	58.9 ± 1.5	11	0.6	3.54 ± 0.25	*16.6 ± 1.5*
								18.1 ± 3.3 (fad. corr.)
		KF, 63–100 μm, $pIRIR_{290}$	CAM	82.9 ± 6.3	10	23.7	3.45 ± 0.27	24.1 ± 2.9
								19.2 ± 2.3 (residual subtracted)

[a] All measurements were carried out on small aliquots (see text for details, the grain size used is indicated in μm) using automated risø TL/OSL readers (type TL-DA-12, -15, or -20, Bøtter-Jensen et al. 2003) with the following settings: Quartz, OSL: detection U340 filter (7.5 mm thickness),pre-heat 10 s @ 240 °C, cut-heat 220 °C TL,50 s @ 125 °C blue stimulation. Quartz, ITL: detection U340 filter (7.5 mm thickness), 500 s @ 310 °C stimulation. K-rich feldspars, $IRSL_{50}$: detection 410 nm interference-filter, pre-heat 10 s @ 270 °C, cut-heat 10 s @ 270 °C, 300 s IRSL @ 50 °C. K-rich feldspars, $pIRIR_{290}$: detection 410 nm interference-filter, pre-heat 60 s @ 320 °C, 200 s IRSL@ 50 °C followed by 200 s IRSL @ 290 °C, after each SAR cycle 100 s IRSL @ 325 °C.
[b] CAM = central age model, MAM = minimum age model (Galbraith et al., 1999).
[c] Number of aliquots used for De calculation.
[d] Overdispersion of the De data set.

In the first instance, the single-aliquot regenerative-dose protocol (SAR) (Murray and Wintle, 2000, 2003; Wintle and Murray, 2006) was applied to all samples in order to attain the equivalent dose (De) values for quartz. All samples, except COS1-3, showed quartz luminescence signals being in saturation or too close to saturation for dating when the standard SAR protocol was used. Hence, alternative approaches were tested for De determination. Only for one sample (ROM1-4a), the isothermal TL (ITL) of quartz (Choi et al., 2006; Jain et al., 2007) yielded reliable results as far as can be deduced from dose recovery tests. A known laboratory dose was reproduced with a ratio (given to the measured dose) of 1.02 ± 0.09 ($n = 4$) measuring the thermoluminescence at a constant temperature of 310 °C and a ratio of 1.09 ± 0.05 ($n = 3$) for a measurement temperature of 270 °C. This independence of thermal treatment and the good dose recovery supported the applicability of the ITL protocol for sample ROM1-4a. Due to the better recovery ratio, a measurement temperature of 310 °C was finally chosen. However, for the other four quartz samples tested, the administered laboratory doses could not be reproduced within an acceptable range of ±10% from unity. Therefore, these samples were not further analyzed by ITL. Instead, the infrared stimulated luminescence (IRSL) of potassium-rich feldspars was used for dating, because the saturation dose of feldspars is much higher than that of quartz from the same sediments. The SAR protocol for K-feldspars was applied as proposed by Wallinga et al. (2000) using the most stable signal component at ~410 nm for dating (Krbetschek et al., 1997). Notwithstanding, these feldspar IRSL emissions, measured with the sample held constantly at 50 °C during IR stimulation (in the following referred to as $IRSL_{50}$), still can show an anomalous signal loss due to the decay of an unstable luminescence signal on laboratory measurement time scales (anomalous fading), that results in age underestimations (e.g. Wintle, 1973; Lamothe et al., 2003). Consequently, samples should be tested for the presence of fading. For samples ROM1-4b and ROM1-5, fading rates were measured according to Auclair et al. (2003), and g-values of 1.9 and 1.6 were obtained for ROM1-4b and ROM1-5, respectively. The ages corrected for fading are shown in Table 4 together with the uncorrected ages. As the applied correction method of Huntley and Lamothe (2001) is considered to be successful for corrections made within the linear part of the dose–response ('growth') curve only, no fading tests were carried out for older samples. $IRSL_{50}$-ages of samples which were not tested and corrected for fading ought to be regarded as minimum ages only, as the occurrence of signal loss since burial cannot be ruled out.

In order to check whether the impact of anomalous fading is serious in the case of the older samples, the approach of post-IR IRSL (pIRIR) dating for K-rich feldspars was tested. We used the measurement protocol as proposed by Thiel et al. (2011, see Table 4). They applied it to polymineral fine grains (4–11 μm) extracted from Austrian loess, but a general applicability to coarse grain K-feldspars has also been shown for example by Buylaert et al. (2009, 2012). The advantage of the $pIRIR_{290}$ (measured at 290 °C) over IRSL (measured at 50 °C) is that the signal, which is finally used for dating, is less affected by fading. Thiel et al. (2011) provided evidence that the $pIRIR_{290}$ signal does not seem to be prone to fading on a time scale of >750 ka, and they considered the low fading rates they had measured for the postIR-IRSL signal to be laboratory artifacts (see also Buylaert et al., 2012). According to these observations and the fact that already the standard $IRSL_{50}$ fading rates were quite low for our Romanian loess samples, we did not carry out any pIRIR fading tests and expect no significant fading of the pIRIR signals. The fact that the $pIRIR_{290}$ signals of numerous sub-samples of ROM1-3 were either saturated or close to saturation (see Fig. 5) supports the hypothesis that the pIRIR signal measured at 290 °C is not affected by anomalous signal loss (fading) over the time period of burial. Four out of nine sub-samples measured for ROM1-3 showed natural $pIRIR_{290}$ signals in saturation or too close to saturation (i.e. $>2^*D_0$, see Wintle and Murray, 2006; see Fig. 5) for reliable determination of equivalent dose values. All other sub-samples of ROM1-3 showed very poor reproducibility with recycling ratios out of the accepted range of 0.9–1.1, whereas the other samples dated by $pIRIR_{290}$ provided good recycling ratios. Therefore ROM1-3 is considered to be not datable by the $pIRIR_{290}$ approach. Hence, severe fading seems to affect the $IRSL_{50}$ signal obtained for the same sample resulting in minimum ages only.

The general applicability of the $pIRIR_{290}$ protocol to the samples investigated in this study was further tested and is supported by the results of a dose recovery test carried out on sample ROM1-4a. After bleaching for 24 h in a Höhnle SOL2 solar simulator, a laboratory dose of 178 Gy was administered, which was recovered by applying the $pIRIR_{290}$ protocol with a ratio of 0.94 ± 0.08 (ratio given/measured dose, $n = 4$). The $pIRIR_{290}$ residual remaining after 24 h of bleaching was also determined on three aliquots. When subtracting this 5.25 Gy, the dose recovery ratio improves to 0.97 ± 0.08.

The bleachability of the pIRIR signal was further tested by measuring aliquots of samples ROM1-4a after 24 h, and of sample ROM1-4b after 1, 6, and 24 h light exposure in the solar simulator. The residuals measured after 1 h light exposure were 16.84 ± 1.72 Gy ($n = 7$, ROM1-4b) or 12.6% of the natural dose, respectively. This residual dose is within the range observed by Thiel et al. (2011) who measured residuals of 15–20 Gy after 4 h bleaching with a solar simulator but with a larger distance between samples and the light source then that used in this study. After 6 h bleaching, the remaining signal was reduced to 6.8% of the natural dose (9.13 ± 1.04 Gy, $n = 3$, ROM1-4b). The residual doses obtained

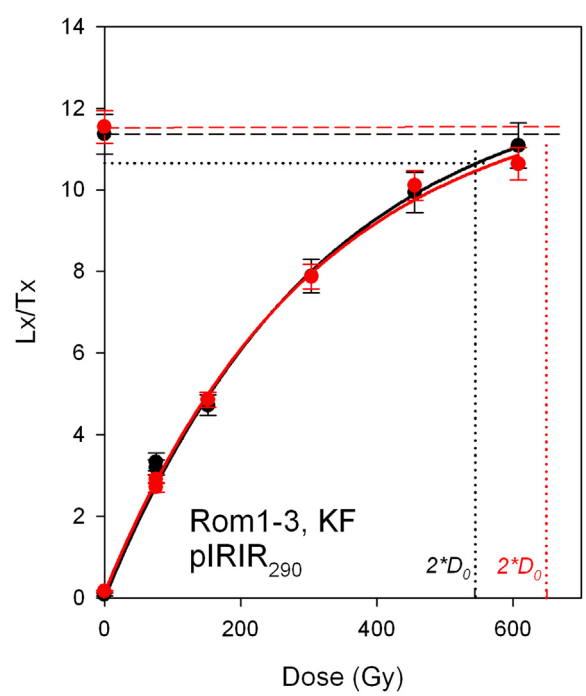

Fig. 5. Representative dose–response curves for pIRIR290 signals obtained on two aliquots of K-rich feldspar extracts from sample ROM1-3. The sensitivity-corrected luminescence signals (Lx/Tx values) are plotted against the laboratory beta dose. Horizontal dashed lines indicate the level of the sensitivity corrected natural pIRIR290 signals. Vertical dotted lines represent the $2D_0$ values. In order to obtain reliable equivalent dose values they should not exceed this value (De < $2D_0$, Wintle and Murray, 2006), i.e. the natural signals should be well below the horizontal dotted line. This is not the case for both aliquots shown here.

after 24 h light exposure for samples ROM1-4a and ROM1-4b are quite similar: for ROM1-4a 5.25 ± 0.71 Gy or 3.2% of the natural dose ($n = 4$) and for ROM1-4b 3.99 ± 1.15 Gy or 3.0% of the De ($n = 5$) (see Fig. S2). These residuals most probably result from an unbleachable $pIRIR_{290}$ signal equivalent to a dose of c. 5 Gy reported by Buylaert et al. (2012). These authors conclude that this residual probably results from thermal transfer. Thus, equivalent doses determined by the $pIRIR_{290}$ protocol are likely overestimating the true depositional dose by about 5 Gy, which becomes less significant with increasing doses or depositional ages, respectively. As a consequence, an unbleachable residual ought to be subtracted from De values before age calculation in order to prevent age overestimation. Thiel et al. (2011) present ages with a residual signal equivalent to 20 Gy subtracted, but they consider the uncorrected ages as being more reliable. Table 4 displays all uncorrected ages together with ages that were calculated from De values of which the residual dose of 16.84 Gy (average residual after 1 h bleaching, see above) was subtracted. Here, for our samples we consider these corrected ages to be more reliable than the uncorrected ones, because within the error boundary, they agree with fading-corrected IRSL ages and the quartz-based ITL age (see Table 4). Finally, the safest interpretation would be to consider the uncorrected ages as maximum ages and the corrected ones as minimum ages.

5. Results

5.1. Sedimentological analysis

For the section Cos 1, the grain size distribution (Fig. 6) shows that silt, making up 50.82% ± 5.42, is the predominant fraction in the whole sequence. By subdividing the silt fraction into fine silt, medium silt and coarse silt, the main silt fraction is medium silt with 18.42% ± 2.84. The second largest fraction of this sequence is fine sand with 29.86% ± 5.06. Clay is subordinately represented with an amount of 16.78% ± 2.74. From the results of grain-size analysis, the section can be divided in three main sedimentary units (Fig. 6):

Unit I: Fine sand predominates and shows a total maximum with around 40%, the highest values for the whole section. Each silt class shows its minimum in this unit. Comparing the results of fine sand using the Fraunhofer and Mie theories (Fig. 7), for fine sand

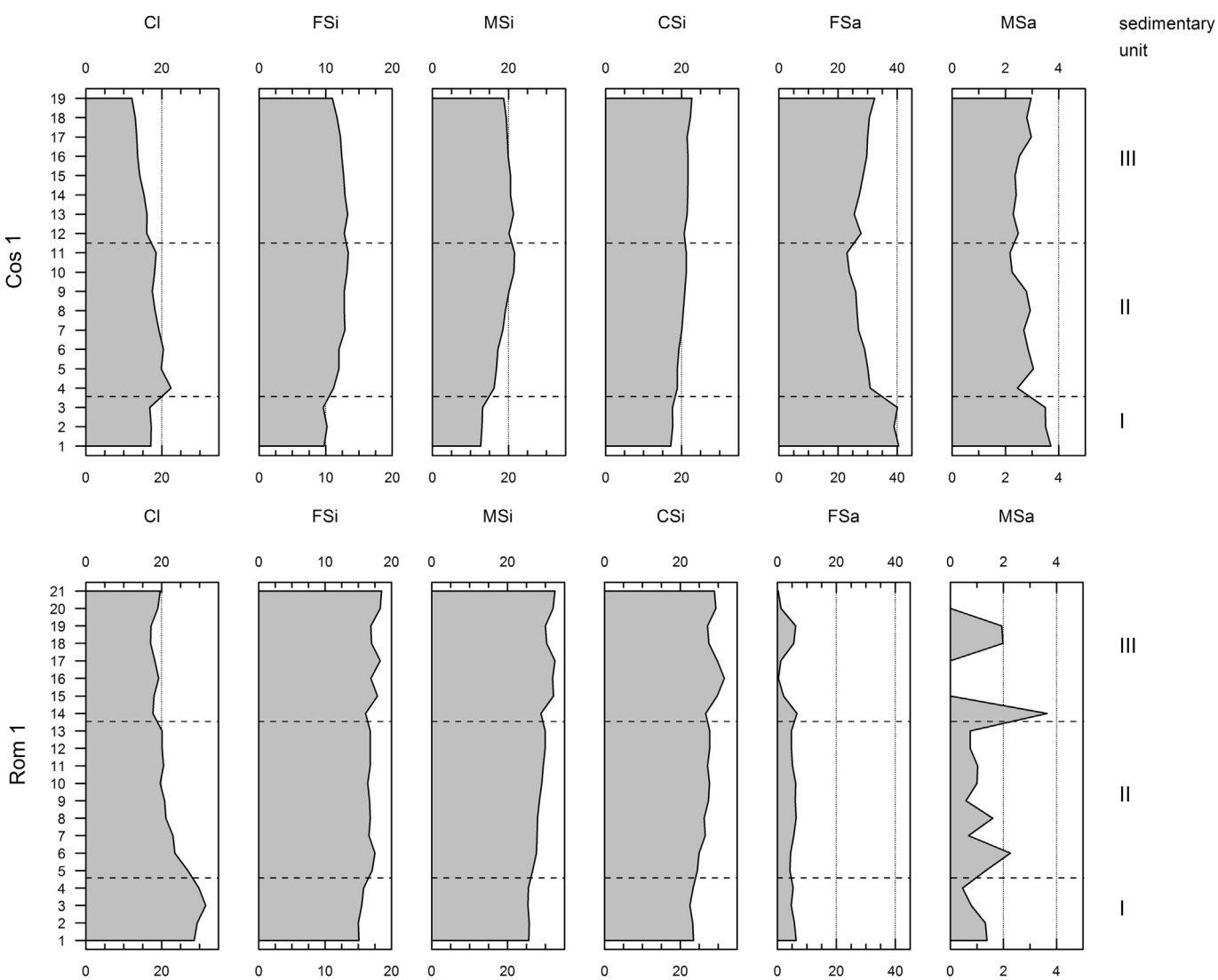

Fig. 6. Grain Size classes (%) for the sections Cos 1 and Rom 1 measured by laser diffraction. Following the ISO International Standard 13320, 2009 the Mie theory for the clay and silt fractions and the Fraunhofer theory for the sand fractions was applied. Cl = clay, FSi = fine silt, MSi = medium silt, CSi = coarse silt, FSa = fine sand, MSa = medium sand.

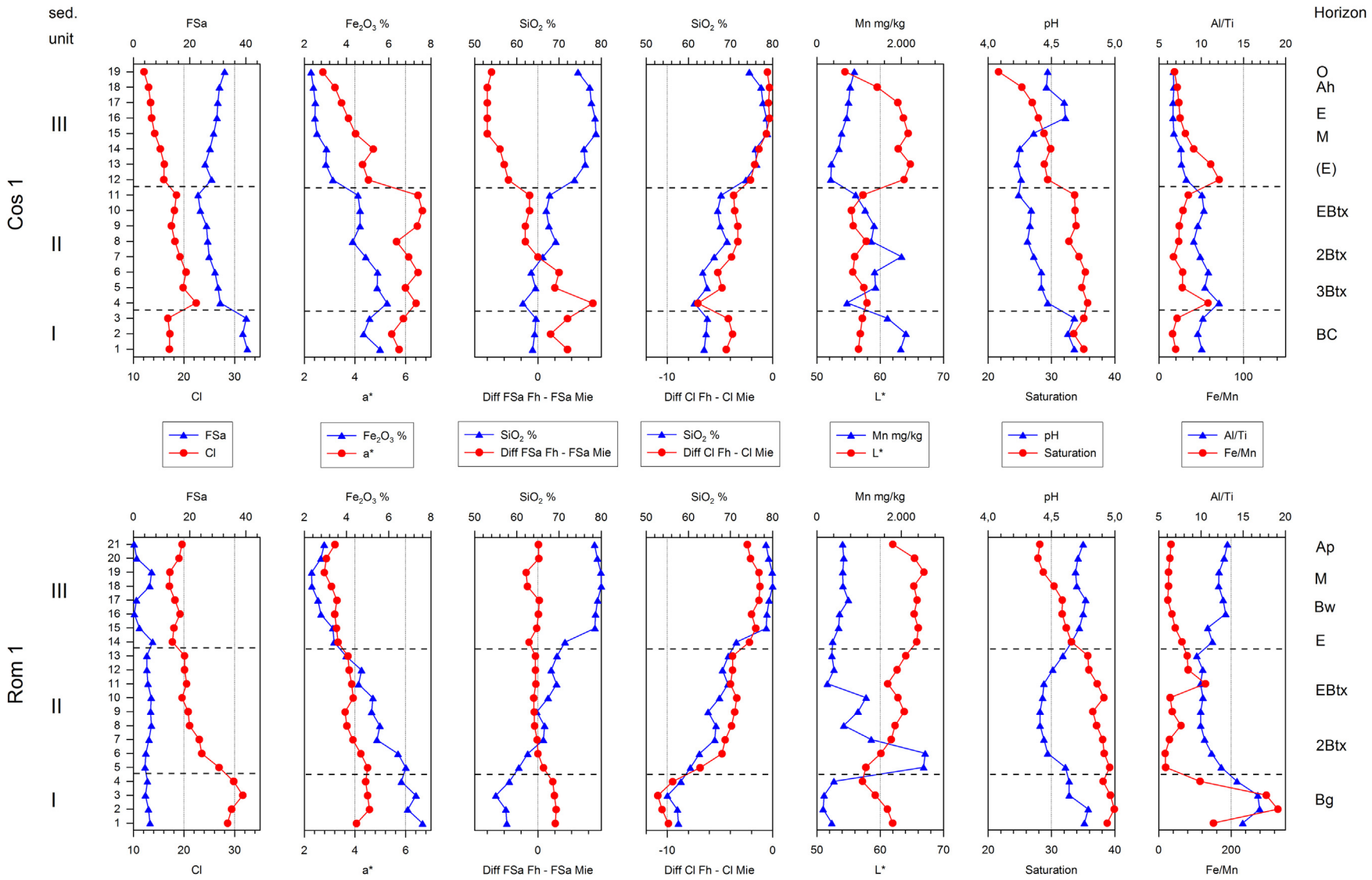

Fig. 7. Analytical results for Cos 1 & Rom 1: Fine sand (FSa) vs. clay (Cl) in %, selected element compositions (%/mg/kg) and ratios; Color values: a^* (red–green), L^* (luminance), Saturation; Diff = differences between the optical models following the theories Fh (Fraunhofer) and Mie; Sed. unit = Sedimentary unit. Apart from the Fe/Mn ratio, all single scales are harmonized for matters of comparability. (For interpretation of the references to color in this figure legend, the reader is referred to the web version of this article.)

the correlation shows a positive correlation with values of up to 0.7. For clay, the differences between the two optical models show a negative trend with a difference of up to 4.8.

Unit II: The fine sand fraction decreases and reaches lowest values with 22%. The clay content attains highest values with 22% at the base and shows a similar trend as the fine sand towards the top of the unit. In contrast, all silt fractions increase. The medium silt shows a maximum of 22% at the top of the unit. Both optical models show a dichotomy of the unit when focusing on fine sand and clay.

Unit III: The content of fine sand increases downwards from the top except at the base of unit III. Silt and clay show a reverse trend with a fine peak and slightly lower values at the base. The other grain size classes are of less importance. They show slight variations of around ±2% on average.

Section Rom1 shows a strong dominance of silt, with a content of 72.64% ± 5.5, which is much higher than that found in Coşava. The main sub-fraction is medium silt with 29% ± 2.39 and coarse silt with 26.85% ± 2.43. The clay content is high with 21.95% ± 4.55. The fine sand plays a minor role with just 4.53% ± 2.1. Three main sedimentary units can be distinguished (Fig. 6):

Unit I: Although the total silt content of almost 64% is high, it represents the lowest value of the whole section. Clay, with an average of 30%, attains the highest amounts for the whole section. The fine sand fraction shows a slightly positive difference by applying the Fraunhofer theory. The difference is more pronounced by using both optical models for the clay fraction (Fig. 7).

Unit II: The silt content increases continuously towards the top up to a value of more than 74%, whereas the clay content, with a mean of 21.73%, is lower than that in unit I. Fine sand is still underrepresented and shows a large deviation. A slight deviation is noticeable for the medium sand fraction. The differences between both optical models (Fig. 7) show similar results for fine sand and decrease in the clay fraction at the beginning, continuing with lower values towards the top of the unit.

Unit III: Each grain size class shows slight deviations. It is possible to define further subdivisions such as the human-induced colluvial layer at the top of this section. In this study, this covering sediment is defined as a single unit. As in Coşava, the sand fraction shows higher values in the basal part in the range of the bleached sediments. In the sediment above the bleached horizon and below the colluviation layer, the silt content increases and attains the highest values of the section with more than 80%. The clay content, with 18.47%, is lower than that in unit II and III. The colluvial layer consists of more fine and medium sand and, consequently, the silt and clay contents decrease slightly. The ploughed horizon shows slightly higher values for these fractions. The differences between the optical models reflect the same trends with slight variations (Fig. 7).

5.2. Luminescence dating

Four samples from the section Cos 1 were dated by luminescence (Fig. 3). According to the $pIRIR_{290}$-age of 202 ± 21 ka and even with respect to the most likely underestimated $IRSL_{50}$-age of 152 ± 15 ka, the sediments represented by sample COS1-1 are of pre-Eemian age. The equivalent dose distributions of samples COS1-2a and -b both show a large spread (Fig. S3), which is unexpected for eolian sediments such as loess (compare radial plots of ROM1-5 in Fig. S1 to radial plots in Fig. S3). Because fossil root channels were observed within the section, it cannot be ruled out that sediments of different ages were intermixed after deposition. The agreement within errors of the $IRSL_{50}$ and the $pIRIR_{290}$ ages obtained for COS1-2b is surprising, given the fact that the IRSL age is not corrected for potential fading. Thus, it should be considered as a minimum age and the pIRIR age – if not been corrected by subtraction of a residual – is regarded as a maximum age. Moreover, the difference in $IRSL_{50}$-ages between COS1-2a and -2b is unexpected, as these two samples were taken from the same stratigraphic layer and should yield comparable ages for sediment deposition. These discrepancies can be attributed to sediment mixing or heterogeneous signal re-setting affecting the equivalent doses. It is not simply a problem of application of various protocols, because the discrepancy is already observed between the two $IRSL_{50}$-ages of 56 ± 6 and 70 ± 7 ka (see Table 4). All De distributions, irrespective of the protocol applied, show an unexpected large scatter (see Fig. S3). However, we conclude that only a rough age estimate can be provided by luminescence dating, i.e. a lower age limit of 56 ± 6 ka ($IRSL_{50}$-age COS1-2a) and of 67 ± 8 ka (uncorrected $pIRIR_{290}$-age of sample COS1-2b).

The broad scatter observed in the equivalent dose distribution of sample COS1-3 most likely results from poor re-setting of the OSL signal during transport (see Fig. S1). Hence, the lowest significant dose component is expected to provide the best dose estimate for the last event of bleaching and, thus, of sediment re-working. The result of the applied minimum age model clearly indicates Holocene re-deposition of the sediments with the event dated most likely to 4.49 (+0.52/−0.47) ka.

At Româneşti, four samples were dated by luminescence (Fig. 4). With a minimum age of 57.9 ± 5.4 ka, the lowermost sample from Rom 1 shows sedimentation dating of MIS 4 or older. As the $pIRIR_{290}$ signals are already saturated or close to saturation, the sediments are most likely even much older. Samples ROM1-4a and -b were taken from the same layer. Three different luminescence approaches were applied and yielded ages with poor agreement. The ITL-age is regarded to be less certain, as the ITL approach showed reproducible results only for this individual sample and might be affected by sensitivity changes which were not fully corrected by the measurement protocol applied here (Buylaert et al., 2006). Nevertheless, the ITL-age is in good agreement with the pIRIR age, even when this is not corrected by subtraction of a residual, both results agree within errors. Taking their uncertainties into account, the fading-corrected $IRSL_{50}$-age of sample ROM1-4b (29.7 ± 5.5 ka) agrees with the corrected $pIRIR_{290}$-age of the same sample (35.5 ± 3.9 ka). The fading correction procedure used here is best suited for a correction of fairly young samples with their dose–response curve still showing linear growth. We consider the fading-corrected IRSL-age to be less reliable than the pIRIR age, because the applicability of the correction procedure is already questionable for sample ROM1-4b. For the younger sample ROM1-5, there is very good agreement between the fading-corrected IRSL-age and the pIRIR age (see Table 4), thereby indicating that the fading correction in this lower dose range seems to work much better.

To summarize, due to the poor agreement within the data, the best age approximation for samples ROM1-4a and -b is the entire time range from 35.5 ka to 45.1 ka. Sample ROM1-5 showed by far the lowest scattering in De values and most likely was not affected by any severe post-depositional disturbances. The fading-corrected $IRSL_{50}$-age dates the deposition of the obviously fully bleached sediments to the final stages of the Last Glacial Maximum at around 18 ka. This date is in very good accordance with the corrected $pIRIR_{290}$-age of 19.2 ± 2.3 ka.

5.3. Geochemical parameters and multielemental analysis

The results of the geochemical analysis are shown in Fig. 7 (selected elements and ratios) and in Fig. S4 (major elements) and Fig. S5 (trace elements). Both sections are completely decalcified and the pH-values are generally low with values ranging from 4.2 to 4.8 (Fig. 6). At Coşava, the pH-values are slightly lower, which

is basically influenced by the acidic, sandy local bedrock sediments. At this location, the tertiary sands and silts display a pH-value of 5.4. Both sections show the same trend for the acidity with an increase towards the bleaching zone and in the upper part of the argillic horizon, decreasing again towards the lower part of the argillic horizon. Although this trend is typical for Albeluvisols in Romania (Mavrocordat, 1971), the conditions at the section Cos 1 are rather acidic in comparison to other measurements on Albeluvisols. Towards the recent surface, the pH-values are slightly higher which illustrates impacts by modern land-use practices.

In both sections, SiO_2, Al_2O_3 and Fe_2O_3 are the major compounds showing similar abundances with depth. The uppermost sediments in unit III at both sites are characterized by an increase in SiO_2 of up to 80% and more, which then considerably decreases with depth with fine deviations in unit II. In contrast, the contents of Fe_2O_3 and Al_2O_3 increase with depth. However, at Cos 1 the argillic horizons are characterized by the highest amounts of Al_2O_3, Fe_2O_3 and MnO whose levels then decrease again in the lowermost unit. This illustrates the higher intensity of weathering, their role as cementing agents in these horizons (Franzmeier et al., 1989; Szymański et al., 2012) and shows a close relation of the abundance of these elements to the grain size distribution, particularly to the clay content.

This relation is even more significant at Rom 1, where the distribution of these elements shows a close relation to the clay contents. As a result, elements with minor abundances like Ti or Mn have to be considered as more reliable weathering proxies. In particular, at Rom 1, the values of MnO show a deviation at the base of unit II where several Mn-nodules are visible within the section, indicating redoximorphic processes combined with an increase in finer grain sizes. The Al/Ti ratio (Fig. 7) reflects the main sedimentary units.

Fe- and Mn-values reflect redoximorphic effects. In general, the mobilization of Fe-compounds is higher under acidic conditions, but increases in loamy soils (Kabata-Pendias, 2011). At a lower pH value below 5, the solubility of Mn increases progressively. Calcareous (not given here) and loamy soils show the highest amounts of Mn, which causes concentric nodules especially in the lower part of the argillic horizon. The amounts of MnO and Fe_2O_3 are shown in Fig. S4. Both compounds show higher values inside the argillic horizon with two weak peaks in both sections. The ratio of Fe/Mn (Fig. 7) represents barriers of limited solubility. This is also visible in a change in grain-size distribution with a higher amount of clay in the range of the argillic horizons that exhibited cemented features during field observation. For both sections, this resulted in a pronounced increase in iron content (Fe_{tot}/Fe_2O_3) at the top of the argillic horizon, causing the reddish to brown color there. In addition, at Româneşti, a higher amount of Fe in relation to Mn appears in the upper part of the groundwater influenced, more grayish horizon at the bottom of the section. Additionally, at Rom 1 the topsoil is considerably enriched with Na_2O because of fertilization.

For both sections, trace elements such as chromium, zinc and rubidium indicate a relationship to finer grain sizes (Fig. S5; Kabata-Pendias, 2011). By comparing the geochemical signatures of Cos 1 and Rom 1, it is clear that soil development there is more or less similar, although both sections developed from different parent sediments. Scatter plots of selected elemental distributions reveal that the samples from the argillic horizon of both sections are located in the same range upon taking into account the respective relationships between MgO to Al_2O_3, Al_2O_3 to TiO_2 and Fe_2O_3 to MnO (Fig. 8).

5.4. Soil color

The results from the soil color measurements generally reflect the main sedimentary units of both sites (Fig. 7). At Cos 1, the a^*-value is comparably high and decreases abruptly with unit III. By

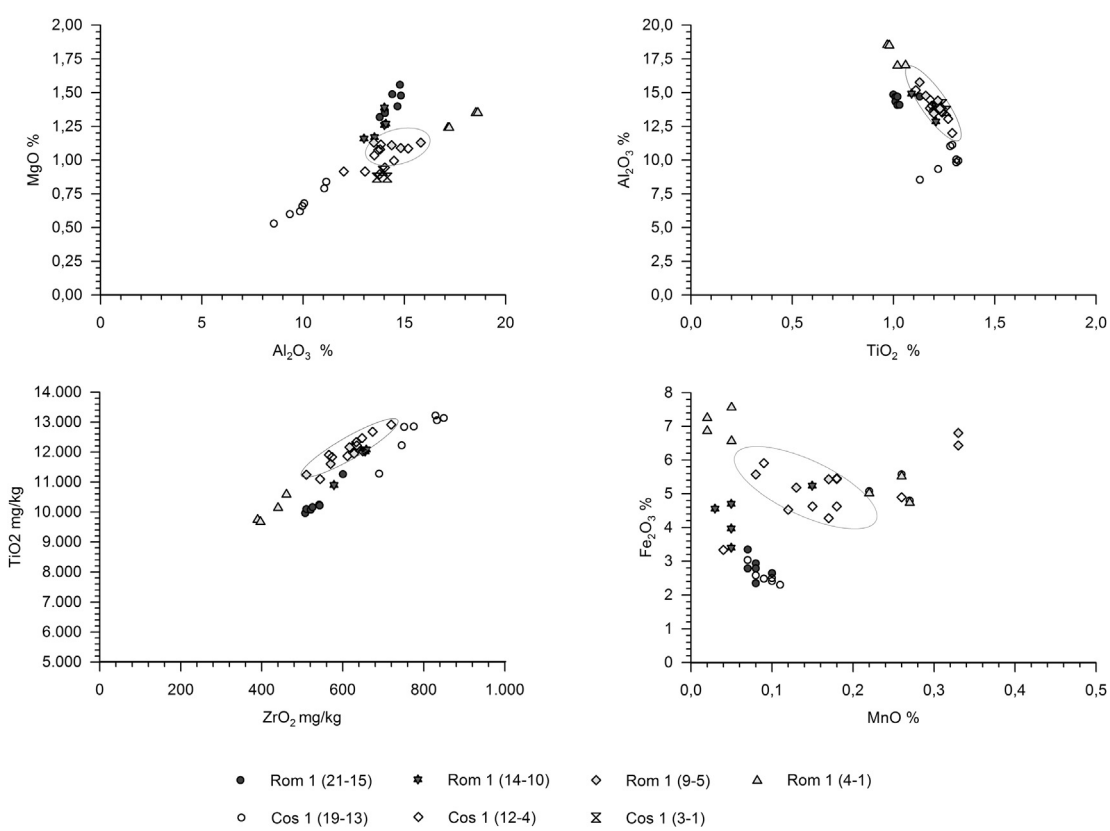

Fig. 8. Scatterplot of selected elements from Rom 1 and Cos 1 (with numbers of samples, see Fig. 3 and 4).

contrast, the luminance (L^* value) is lower in unit I and II and increases in unit III until it decreases again in the humic horizon. The saturation increases with depth from unit I to II. Color measurements at Rom 1 show the same trend with different intensities. The a^*-value decreases with slight deviations; the L-values are higher but reflect the main units. Moreover, the saturation decreases more or less continuously with fine deviations.

6. Discussion

6.1. Sedimentary development and pedogenetic processes

The combination of results from field observation, luminescence dating as well as from sedimentary and geochemical analyses shows that the genesis of the soil system is rather complex and the soil development is polygenetic. Even though the sections Rom 1 and Cos 1 look similar from an initial macroscopic point of view, they differ with respect to the parental sediments, the sedimentation history and the pedogenesis.

First, the different geomorphological positions affect the sediment composition and soil development. As the slope of the plateau spur of the Coşava site is steeper than the slope aspect of the Româneşti site, reworking processes have been more intense at that site. With regard to Coşava, this is reflected by coarser grain-size and more isolated pebbles that originate from the gravel layer as well as by several discordances. By contrast, the Româneşti site is situated on a relatively flat plateau. Features including sand stripes, layering of sediments and a higher amount of single pebbles throughout the section, which would be characteristic for reworked sediments are not obvious. Thus, it can be concluded that denudation effects were not as intense at Româneşti as in Coşava.

Second, the basal part (unit I) is quite different at both sites. At Coşava this is the sandiest part of the section, which is influenced by the sediments exposed close to the surface at the whole plateau spur. The basal groundwater-influenced unit at Româneşti is very rich in clay. These sediments here may belong to former floodplain sediments of the Bega terrace. As the differences between both optical models are significant for this unit, we suggest a different parental material in comparison with that of the covering sediments (unit II and III). More important for the understanding of the genesis of soil and sediment is the kind of weathering which affected the sections and which ought to be characteristic for comparable morphological positions, as we observed similar soil features in the study area at the foothills of the Banat Mountains.

The upper part of unit II is equal at both sections with two dense horizons, whereas the upper half is spotted with rust and fine concretions of iron oxides and the lower half is enriched with manganese nodules. Cos 1 differs in the lower part of this unit, because there is a second dense horizon which is partly eroded. Both sections show comparably high amounts of clay throughout this unit, especially in the lower part. Field observations confirm that this clay enrichment shows no intense clay cutans as a result of pedogenesis by a Luvsiol, but more or less strong clay coatings. How can one understand the genesis of the increase in clay in the middle part (unit II) of the sections? As evidence for chemical weathering, silica has to be released and accumulated in the subsoil, where binding with Fe_2O_3 and clays should be apparent (Bockheim and Hartemink, 2013). SiO_2 decreases rapidly with the bleaching horizon and in unit II, whereas the amounts of Fe_2O_3 and MnO increase with slight deviations. These processes are impressively reflected by the soil color with lower luminance and an increase in saturation towards unit II. Beneath that, some trace elements such as Cr, Zn and Rb reflect higher amounts of finer fractions (Fig. S5). Thus, the decrease in grain sizes, resulting in a denser horizon in unit II, is attributed to chemical weathering caused by hydrolysis.

In both sections, this unit is connected to the Aurignacian level. Inside this unit, several levels of fossil root channels occur. Even if they might be eroded slightly, they indicate a former existence of stable surfaces and of higher vegetation with shrubs and trees. Therefore, there are probably remnants of fossil soil development of interstadial character (at least weak A-soils). As tested by multielemental analysis, there are no clear indications of such soils in unit II. However, this might be influenced by the strong, overprinting pedogenesis of the surface soil.

Intense bleaching is documented for both sections with the beginning of unit III. Whereas the bleached horizon is still preserved in its original context at Rom 1, at Cos 1 it has undergone complete erosion so that only infillings of root channels in the underlying argillic horizon testify its former presence (top of unit II, samples 12 and 13).

The amount of SiO_2 decreases rapidly within the argillic horizons. Toward the top (unit III) and in comparison with the overlaying sediments, the SiO_2 content is remarkably higher, already increasing within the bleached horizons, caused by eluviation processes. Parallel to that, the amounts of Al_2O_3 increase through the sections from the top towards the bottom. In unit II, the change in the grain size with higher amounts of clay is a result of stronger weathering processes.

Another secondary process was the release of Fe and Mn linked to the more or less intense stagnic features which appeared during and after the formation of the argillic horizons. It still remains open whether the effects of weathering and secondary stagnic processes destroyed initial and weak interstadial soil development with at least weak pre-weathered sediments.

Regarding all the phenomena described above, these dense argillic horizons show features of a fragipan. In general, fragipan soils are described as a rather dense subsurface soil horizon, which causes limited infiltration of water and restricts the penetration depth of roots (Soil Survey Staff, 2010). They are characterized by a thickness of more than 15 cm, a coarse prismatic structure, and a very hard consistency. As they do not contain major amounts of organic carbon or carbonates, they do not result from secondary cementation.

Fragipan genesis is a controversial topic, possibly because this horizon can develop under different conditions in various archives such as loess, colluvial deposits, lacustrine sediments, till, or alluvium (Witty and Knox, 1989). On the one hand, there are numerous studies indicating that fragipans developed under periglacial climatic conditions together with permafrost action (Payton, 1992; Van Vliet-Lanoë, 1998; Driessen et al., 2001). On the other hand, the formation of a fragipan can take place under more moderate and humid climate conditions (Franzmeier et al., 1989).

The experiments on fragipans by Attou and Bruand (1998) support the idea that fragipans developed under different climatic conditions and that successive wetting and drying cycles are one reasonable explanation. During a wetting period, a dispersion of fine material can promote a clay-particle accumulation which, during a following drying period, is reorganized to form clay-bridges and clay-coatings.

With this and through degradation processes during seasonal drying, vertical cracks (albeluvic tongues) can be developed and later filled with bleached surface soil material. Furthermore, high clay contents and iron–manganese nodules are often related to such fragic horizons (Szymański et al., 2011, 2012). This current paper argues, however, that the dense horizons of both sections with fragic features did not develop through permafrost, because there are no signs for such structures as described above. Here, the processes lead to fragic features which are related to the dense and cemented argillic horizons of our two sections and occur in the frame of the development of Albeluvisols. As observed during several prospections at the foothills of the Banat Mountains, we

assume a wider distribution of fragic horizons in comparable altitudes and morphological positions along the Carpathian arc than were expected as yet.

Modern human activities had affected the ongoing soil-forming processes. The decreased pH-values below the colluvial layers of unit I and into unit II are linked to land use. At Rom 1 the pH-value increases continuously towards the top of the section which is regarded as a result of modern tillage. By contrast, at Cos 1 this increase is reversed in the topmost samples, possibly indicating fire clearance to keep pastures open, which is still usual in this region nowadays. Expecting that these effects should promote a lowering of the pH value, we suggest that there ought to be no intense clay illuvation today and that the main processes which caused the argillic horizons ended.

6.2. Chronostratigraphy and Upper Paleolithic industries

In Coşava I, findings of archeological level I are connected on top or inside of the lowermost fragic horizon. Due to the intensity, this horizon was formerly interpreted as remnants of an interglacial soil (Sitlivy et al., 2012, in this volume). As we obtained a pre-Eemian age of the lowermost luminescence sample (COS1-1: 202 ± 2 ka) below that horizon and an early glacial age of the samples in the middle part of the sequence (COS1-2a and -b: 56–61 ka), it is surprising that especially the findings of the lowermost archeological level I and of the deeper part of archeological level II, beneath these two luminescence ages, show typical Upper Paleolithic features. Therefore, it is more likely that the lowermost findings are situated in reworked sediments and that, here, grains were not fully exposed to daylight and the luminescence signal not completely reset. The difficulties in dating these samples and the large discrepancies between two samples from the same layer illustrate the problems with signal resetting.

Even though more precise age estimates are missing for the upper part of archeological level II, thin sedimentation of loess-like sediments has continued and covers the former reworked layers. At the moment, it cannot be ultimately solved if at least some findings from here are positioned more or less *in situ*. Further dating of this part of the sequence would be necessary. In comparison to the Româneşti sequence, here is an obvious increase in clay content, regarded as an effect of weathering. With the beginning of archeological level III, there is a discordance as exhibited in the change in sedimentation, the increase of single pebbles, the missing of a bleached layer (which is just conserved in tongues) and a colluvial deposit with a minimum age of 4.4 (+0.5/−05) ka BP (COS1-3, OSL, quartz). This shows that the artifacts with features of Upper Paleolithic tradition are strongly reworked here.

In contrast to Coşava, the Româneşti site differs in several ways such as in morphological position, finer sediment, slightly dissimilar soil development, and a larger amount of separate archeological horizons (Sitlivy et al., 2012). For Româneşti I, the lowermost quartz industry (level I, belonging to GH 4) is separated from the Aurignacian layers. Unfortunately, we could not provide age estimates for the lowermost sediments sampled for luminescence dating. The uncorrected $IRSL_{50}$-age of 57.9 ± 5.4 ka represents the minimum value, whereas the $pIRIR_{290}$ measurements indicate potentially much older burial ages. Even if the luminescence data of this part with an age of 57.9 ± 5.4 ka are imprecise, artifacts may be dated younger than the last interglacial complex, but older than the last interstadial period. Although parts of the section show fine discordances, the Aurignacian assemblages from GH 3 most likely date to MIS 3, with ages of between 35.5 and 45.1 ka (ROM1-4a, -b) from the middle part of this section.

Based on the $pIRIR_{290}$-age range presented for the sediments in that zone (sample ROM1-4a and -4b: 35.5-45.1 ka), the formation of the fragipan could have begun during MIS 3, but at the latest during MIS 2. For a more precise temporal estimation of this process, further investigations are necessary.

Above the fragic horizon and from the sediment belonging to the bleaching zone in Rom 1, we obtained an age at the end of the last glacial cycle (18.1 ± 3.3 ka or 19.2 ± 2.3 ka, respectively, Table 4). Towards the top of the section Rom 1 and from the lower part of the sediments of GH 2 the luminescence age of 19.2 ± 2.3 ka dates loess sedimentation during the Upper Pleniglacial (MIS 2), which fits to the archeological level with Gravettian inventory. The brownish colluvial horizon in Cos 1, above the remnants of the bleached horizon and the most intense bleached tongues, is dated to the mid-Holocene: 4.49 (+0.52/−0.47) ka. This bleaching and, thus, the development of a surface soil regarded to be an Albeluvisol occurred between the end of the last glacial period and mid-Holocene. An initial development of Albeluvisols from Late Glacial on is reported from Germany (Kühn et al., 2006). Although the sediments sampled for luminescence dating turned out to be challenging, especially because they were affected by saturation and/or reworking resulting in inhomogeneous resetting of the luminescence signals, we consider our luminescence chronology as a first age assessment for the sediments investigated here. In particular, analysis of the fine grain (4–11 μm) quartz fraction might help to overcome saturation of the quartz signal and to limit the scattering in De values (e.g. Constantin et al., 2012; Kreutzer et al., 2012). Problems caused by residual signals can be minimized with better bleachability of the quartz luminescence signal compared to the $pIRIR_{290}$ signal of K-rich feldspars. The size of residuals is difficult to define for natural samples as long as no modern analogue is available and even more challenging or even impossible for reworked deposits. Regarding the archeological perspective, it has to be pointed out that the Aurignacian layers are linked to MIS 3, although reworking processes cannot be excluded. As shown, the latter is more likely the case for the Coşava site.

6.3. Paleoenvironmental and paleoclimatic interpretation

Last Glacial sediments at the Banat foothills of the Carpathian Mountains containing paleolithic finds have been dated by luminescence techniques for the first time. With the sediments located in the same region but developed on two different morphological positions, the results from granulometry and geochemistry offer both a brief view on sedimentary evolution and hints about the soil development. Summarizing these aspects, this current study has provided first insights into paleoenvironmental and paleoclimatic history. Although the sedimentary cover with features of loess-like sediments and loess is thin and shows at least some phases of erosion, a general picture can be given as follows:

1. MIS 6: As attested at Coşava, there is a local sedimentation on morphological steps. Here, the sediments show features of the parent Neogene sediments. At Româneşti, there has been no age control for sediments of that time-slice.
2. MIS 5: As detected by field observations, there are hints of a weathered horizon that might belong to the last interglacial period at Coşava. Interstadial soils are expected, but cannot be recognized analytically at present.
3. MIS 4: During the Lower Pleniglacial, there is local sedimentation at both sites. The thin gravel layer, which can be found all over the plateau in Coşava, is seen as an important erosional phase which might have happened with the beginning of the Lower Pleniglacial. The oldest Paleoltihic occupation at Româneşti (quartz industry) could belong to that period or is slightly older.
4. MIS 3: At both sites, the sedimentation continued during the Middle Pleniglacial. Embedded in these sediments are the layers

with Aurignacian findings. Even though it is possible that the formation of the fragipan already began during that time, clear interstadial fossil soil developments cannot be confirmed. Different levels of fossil root channels here indicate at least phases with higher vegetation, which might be a type of forest-steppe.

5. MIS 2: Covering sediments of the Upper Pleniglacial inhibit Gravettian findings at Româneşti. Here, changes in grain-size distribution reflect new sedimentation with higher amounts of silt. Although glacial conditions have to be expected for this period, there is no evidence of permafrost conditions including periglacial features such as ice-wedge pseudomorphs, cryoturbation, or solifluction. Bleaching of the sediments has to be seen as a secondary soil development process. However, it is still uncertain whether this process had already started during Late Glacial.
6. MIS 1: At least during the Holocene, the original sediments were subjected to intense weathering that resulted in a decrease in the pH-value and in the SiO_2 content as well as an increase in the Al_2O_3 content. This caused the development of the argillic horizon in the middle parts of both sections. Linked to that is a bleaching in the upper part of the soil sections. The argillic horizon, which might has overprinted former features of a fragipan masks the levels of Aurignacian findings at both sites. As another secondary effect, stagnic properties are common. Thin packages of colluvial deposits from the Holocene can be found at both sites. At Româneşti, they are anthropogenic and include pottery of different times. The land use was dissimilar at both sites: whereas Coşava was covered by forest and grassland, tillage has been a traditional practice at Româneşti (ploughed horizon). There, the low pH-values below the colluvial layer point to fire clearance to keep pastures open, which is still a common practice in the region.

For the paleoenvironmental reconstruction, there are no hints as yet that the region was affected by permafrost conditions during glacial stages. Because of the occurrence of Aurignacian layers, a special focus is placed on unit II with sediments belonging to MIS 3 and 2. From here, interstadial soils should be expected, but cannot be recognized analytically at present. This may be attributed to the strong weathering which strongly affected the sediments, resulting in a fragipan and a Holocene surface soil that is a stagnic Albeluvisol. As tested, there is no preservation of pollen in the range of such strongly weathered soils. Nevertheless, presence of higher vegetation in the range of unit II is apparent by several levels of fossil root channels. Thus, at least a forest steppe is implied at the foothills of the Carpathian Mountains during MIS 3. This is in contrast to the Pannonian Basin further to the west, where grassland was the dominating type of vegetation on loess apart from wetland areas (Zech et al., 2009). Therefore we suggest, that the foothills of the Carpathian Mountains occurred as a refuge area for higher vegetation during the last Middle Pleniglacial.

It is assumed that the most important climate factor for these changes in paleoenvironment must have been a higher amount of precipitation close to the mountain range in comparison to the drier Pannonian Basin in the west. To summarize, the foothills of the Banat Mountains might have offered a more favorable landscape for the settlement of early modern humans, reflected by the higher density of confirmed findings in the region.

7. Conclusion

This study presents a first deeper insight into chronostratigraphy and the development of last glacial loess-like sediments that comprise Upper Paleolithic assemblages in the foothills of the Banat Mountains. The combination of grain-size analyses and geochemistry shows the development of sedimentation and soil genesis in a higher resolution.

The Paleolithic sites of Româneşti and Coşava are embedded in silty (loess-like) sediments of Last Glacial cycle. Apart from the more or less strong effects of erosion in both sections, the results from luminescence dating support the thesis of sedimentary evolution. The sediments from the main archeological concentrations with Aurignacian features, which are linked to the settlement of early modern humans, the main focus of our research, belong to the Middle Pleniglacial (MIS 3) at the section Rom 1. The site of Coşava was affected by stronger phases of erosion but offers Aurignacian levels above sediments dated to late MIS 4/beginning of MIS 3. The development of interstadial fossil soils during MIS 3 cannot be recognized analytically at present. We could not precisely date the fossil root channels; at least the ones of the upper part within the weathered horizons might have been developed during Holocene. Moreover, deeper fossil root channels could possibly belong to MIS 3, as OSL ages of the sediments on top and below attest. If this assumption is true, fossil root channels connected to the MIS 3 indicate a higher vegetation cover that ought to be related to a higher amount of precipitation than that of the lowlands further to the west. Local vegetation and climate factors might have driven the presence of early modern humans in the region during Middle Pleniglacial.

To elucidate the whole site formation process, we focused on the polygenetic history of the surface soil which is a stagnic Albeluvisol here and in comparable morphological positions of the region. This soil inhibits a rather dense weathering zone with features of a fragipan, overprinting the Aurignacian levels. However, the genesis of this weathered horizon is not attributed to permafrost processes. The main weathering processes led to a reduction in the grain sizes within the fragic horizons. Connected to the formation of these dense horizons, secondary effects took place and caused stagnic features. An ongoing release of Fe and Mn was the result of bleaching on top of the argillic horizons. A decrease in the pH-values is attributed to the slash-and-burn land use. All these processes occurred during the development of Albeluvisols. A wider distribution of such fragic horizons is assumed for hillside positions along the Carpathian arc.

Acknowledgements

The investigations were carried out in the context of the CRC 806 “Our way to Europe”, subproject B1 “The Eastern Trajectory”: “Last Glacial Paleogeography and Archeology of the Eastern Mediterranean and of the Balkan Peninsula”, supported by the DFG (Deutsche Forschungsgemeinschaft). Logistical support for the Romanian team was also provided by the National Council of Scientific Research for Higher Education (CNCSIS) through the research grant ID_628.

The authors are grateful to Andrey Veselsky, Cristian Ţuţu and Thomas Felauer for supporting the fieldwork and the excavations in 2009, always accompanied by fruitful discussions.

We like to thank Eileen Eckmeier, Loredana Niţă and Thorsten Uthmeier for helpful comments on an earlier version of the manuscript. Finally, we would also like to thank János Kovács and one anonymous reviewer for their inspiring and constructive comments on the manuscript.

Appendix A. Supplementary data

Supplementary data related to this article can be found at http://dx.doi.org/10.1016/j.quaint.2014.04.063.

References

AG Boden, 2005. Bodenkundliche Kartieranleitung, Hrsg.: Bundesanstalt für Geowissenschaften und Rohstoffe in Zusammenarbeit mit den Staatlichen Geologischen Diensten, fifth ed. Hannover, 438 pp.

Anghelinu, M., Niţă, L. What's in a name: the Aurignacian in Romania. Quaternary International. http://dx.doi.org/10.1016/j.quaint.2012.03.013 (in this volume).

Anghelinu, M., Niţă, L., Sitlivy, V., Uthmeier, T., Băltean, I., 2012. Looking around Peştera Cu Oase: the beginnings of Upper Paleolithic in Romania. Quaternary International 274, 136–157.

Attou, F., Bruand, A., 1998. Experimental study of 'fragipans' formation in soils. Role of both clay dispersion and wetting-drying cycles. Comptes Rendus de l'Academie des Sciences Series IIA Earth and Planetary Science 326 (8), 545–552.

Auclair, M., Lamothe, M., Huot, S., 2003. Measurement of anomalous fading for feldspar IRSL using SAR. Radiation Measurements 37, 487–492.

Blott, S.J., Pye, K., 2012. Particle size scales and classification of sediment types based on particle size distributions: review and recommended procedures. Sedimentology 59, 2071–2096.

Bockheim, J.G., Hartemink, A.E., 2013. Soils with fragipans in the USA. Catena 104, 233–242.

Bøtter-Jensen, L., McKeever, S.W.S., Wintle, A.G., 2003. Optically Stimulated Luminescence Dosimetry. Elsevier, Amsterdam, p. 374.

Buurman, P., Pape, Th, Muggler, C.C., 1997. Laser grain-size determination in soil genetic studies 1. Practical problems. Soil Science 162, 211–218.

Buylaert, J.P., Murray, A.S., Huot, S., Vriend, M.G.A., Vandenberghe, D., De Corte, F., Van den Haute, P., 2006. A comparison of quartz OSL and isothermal TL measurements on Chinese loess. Radiation Protection Dosimetry 119, 474–478.

Buylaert, J.P., Murray, A.S., Thomsen, K.J., Jain, M., 2009. Testing the potential of an elevated temperature IRSL signal from K-feldspar. Radiation Measurements 44, 560–565.

Buylaert, J.P., Jain, M., Murray, A.S., Thomsen, K.J., Thiel, C., Sohbati, R., 2012. A robust feldspar luminescence dating method for Middle and Late Pleistocene sediments. Boreas 41 (3), 435–451.

Băltean, I., 2011. The Palaeolithic in Banat. In: Draşovean, F., Jovanović, B. (Eds.), The Prehistory of Banat, The Palaeolithic and Mesolithic, Bucureşti, vol. 1, pp. 19–76.

Cârciumaru, M., 1978. Paleoliticul din Banat. Cu un studiu paleoclimatic si geocronologic. Academia de stiinte sociale si politice a republich socialiste Romania. Institutul de arheologie, Bucuresti, bibliotheca de arheologie, XXXII, Bucureşti, pp. 83–105.

Cârciumaru, M., 1989. Contexte stratigraphique, paléoclimatique et géochronologique des civilisations du Paléolithique Moyen et Supérieur en Roumanie. L'anthropologie 93 (1), 99–122.

Chirica, V., 1996. Les habitats de Banat. In: Chirica, V., Borziac, I., Chetraru, N. (Eds.), Gisements du Paléolithique supérieur ancien entre le Dniestr et la Tissa. B. A. I. V. Helios, Ias, i, pp. 125–138.

Choi, J.H., Murray, A.S., Cheong, C.S., Hong, D.G., Chang, H.W., 2006. Estimation of equivalent dose using quartz isothermal TL and the SAR procedure. Quaternary Geochronology 1, 101–108.

Commission Internationale de l'Eclairage, C.I.E., 1978. Recommendations on Uniform Color Spaces, Color-difference Equations, Psychometric Color Terms. – Supplement No. 2 of publication CIE No. 15 (E-1.3.1). Bureau Central de la CIE, Paris, 21 pp.

Conea, A., 1969. Profils de loess en Roumanie. In: Fink, J. (Ed.), La stratigraphie des loess d'Europe, Bulletin de l'Association française pour l'étude du Quaternaire, Suppl. INQUA, pp. 127–134.

Conea, A., Bally, R., Canarache, A., 1972. Guidebook to Excursion of the Inqua Loess Symposium in Romania, 11–15 September 1972. Geological Institute, Guidebooks to excursions, 10, Bucharest, 54 pp..

Constantin, D., Timar-Gabor, A., Veres, D., Begy, R., Cosma, C., 2012. SAR-OSL dating of different grain-sized quartz from a sedimentary section in southern Romania interbedding the Campanian Ignimbrite/Y5 ash layer. Quaternary Geochronology. http://dx.doi.org/10.1016/j.quageo.2012.01.012.

Driessen, P., Deckers, J., Spaargaren, O., Nachtergaele, F., 2001. Lecture Notes on the Major Soils of the World. World Soil Resources Reports No. 94, FAO, 344 pp..

Duller, G.A.T., 2008. Single-grain optical dating of Quaternary sediments: why aliquot size matters in luminescence dating. Boreas 37, 589–612.

Eshel, G., Levy, G.J., Mingelgrin, U., Singer, M.J., 2004. Critical evaluation of the use of laser diffraction for particle-size distribution analysis. Soil Science Society of America Journal 68, 736–743.

FAO, 2006. Guidelines for Soil Description, fourth ed. FAO (Food and Agriculture Organization of the United Nations), Rome. 97 p.

Florea, N., Asvadurov, H., Cioflica, G., 1966. Consideratii paleogeografice pe baza profilului cuarternar de la Semlac (Cimpia Tisei). In: Dari de seama, Inst. Geol., vol. LII (1964-1965), I-a, pp. 443–460.

Franzmeier, D.P., Norton, L.D., Steinhardt, G.C., 1989. Fragipan Formation in Loess of the Midwestern United States. In: Smeck, N.E., Ciolkosz, E.J. (Eds.), Fragipans: Their Occurrence, Classification, and Genesis, Soil Science Society of America Special Publication 24, pp. 69–112.

Galbraith, R.F., 1988. Graphical display of estimates having differing standard errors. Technometrics 30 (3), 271–291.

Galbraith, R.F., Roberts, R.G., Laslett, G.M., Yoshida, H., Olley, J.M., 1999. Optical dating of single and multiple grains of quartz from Jinmium Rock Shelter, Northern Australia: part I, Experimental design and statistical models. Archaeometry 41, 339–364.

Gâstescu, P., Pisota, I., Ciovica, N., Patachie, I., 1975. The hydro-climatic particularities of Romania (Hydroklimatische Besonderheiten Rumäniens; les particularités hydro-climatiques de la Roumanie). Geoforum 6 (1), 29–37.

Hahn, J., 1970. Recherches sur l'Aurignacien en Europe centrale et orientale. L'Anthropologie (Paris) 74, 195–220.

Hahn, J., 1977. Aurignacien, das ältere Jungpaläolithikum in Mittel- und Osteuropa. In: Fundamenta: Reihe A, Bd. 9. Böhlau, Köln, Wien.

Hilgers, A., Murray, A.S., Schlaak, N., Radtke, U., 2001. Comparison of Quartz OSL Protocols using Late Glacial and Holocene dune sands from Brandenburg, Germany. Quaternary Science Reviews 20, 731–736.

Huntley, D.J., Lamothe, M., 2001. Ubiquity of anomalous fading in K-feldspars and the measurement and correction for it in optical dating. Canadian Journal of Earth Sciences 38, 1093–1106.

Ianoş, G., 2002. General considerations on the soil cover of Banat (Romania). Geographica Pannonica 6, 13–16.

ISO 13320, 2009. International Standard ISO 13320 – Particle Size Analysis – laser Diffraction Methods. International Organization for Standardization, Geneva.

ISO 14688, 2002. International Standard ISO 14688 – Geotechnical Investigation and Testing – Identification and Classification of Soil. Part 1: Identification and Description. International Organization for Standardization, Geneva.

IUSS Working Group WRB, 2007. World Reference Base for Soil Resources 2006, First Update 2007. A Framework for International Classification, Correlation and Communication, second ed. World Soil Resources Reports No. 103, FAO, Rome.

Jain, M., Murray, A.S., Bøtter-Jensen, L., 2007. Dose response, thermal stability and optical bleaching of the 310°C isothermal TL signal in quartz. Radiation Measurements 42, 1285–1293.

Jarvis, A., Reuter, H.I., Nelson, A., Guevara, E., 2008. Hole-filled Seamless SRTM Data V4. International Centre for Tropical Agriculture (CIAT). Available from: http://srtm.csi.cgiar.org.

Kabata-Pendias, A., 2011. Trace Elements in Soils and Plants, fourth ed. 520 pp.

Krbetschek, M.R., Götze, J., Dietrich, A., Trautmann, T., 1997. Spectral information from minerals relevant for luminescence dating. Radiation Measurements 27 (5/6), 695–748.

Kreutzer, S., Fuchs, M., Meszner, S., Faust, D., 2012. OSL chronostratigraphy of a loess-palaeosol sequence in Saxony/Germany using quartz of different grain sizes. Quaternary Geochronology 10, 102–109.

Kühn, P., Billwitz, K., Bauriegel, A., Kühn, D., Eckelmann, W., 2006. Distribution and genesis of Fahlerden (Albeluvisols) in Germany. Journal of Plant Nutrition and Soil Science 169 (3), 420–433.

Lamothe, M., Auclair, M., Hamzaoui, C., Huot, S., 2003. Towards a prediction of long-term anomalous fading of feldspar IRSL. Radiation Measurements 37, 493–498.

Marković, S.B., Bokhorst, M.P., Vandenberghe, J., McCoy, W.D., Oches, E.A., Hambach, U., Gaudenyi, T., Jovanovi, M., Zöller, L., Stevens, T., Machalett, B., 2008. Late Pleistocene loess-palaeosol sequences in the Vojvodina region, north Serbia. Journal of Quaternary Science 23 (1), 73–84.

Mavrocordat, G., 1971. Die Böden Rumäniens, Giessener Abh. z. Agrar- und Wirtschaftsforsch. d. Europ. Ostens 58, 155 S.; 36 Taf. Duncker and Humblot, Berlin.

Mogoşanu, F., 1972. Information générale sur le paléolithique du Banat (sud-ouest de la Roumanie). Dacia N. S. XVI, pp. 5–27.

Mogoşanu, F., 1978. Paleoliticul din Banat. Cu un studiu paleoclimatic şi geocronologic. Academia de ştiinţe Sociale şi Politice a Republicii Socialiste România. Institutul de Arheologie Bucureşti. XXXII: 152 p.; Bucureşti.

Munteanu, I., Florea, N., 2001. Present-day status of soil classification in Romania. In: Micheli, E., Nachtergaele, F.O., Jones, R.J.A., Montanarella, L. (Eds.), Soil Classification 2001. European Soil Bureau Research Report 7, pp. 55–62.

Murray, A.S., Wintle, A.G., 2000. Luminescence dating of quartz using an improved single-aliquot regenerative-dose protocol. Radiation Measurements 33, 57–73.

Murray, A.S., Wintle, A.G., 2003. The single aliquot regenerative dose protocol: potential for improvements in reliability. Radiation Measurements 37, 377–381.

Özer, M., Orhan, M., Isik, N.S., 2010. Effect of particle optical properties on size distribution of soils obtained by laser diffraction. Environmental and Engineering Geoscience XVI (2), 163–173.

Payton, R.W., 1992. Fragipan formation in argillic brown earths (Fragiudalfs) of the Milfield Plain, north-east England. I. Evidence for a periglacial stage of development. Journal of Soil Science 43, 621–644.

Posea, G., 1975. The relief of Romania as a theme in geographical research. Geoforum 6 (1), 21–27.

Prescott, J.R., Hutton, J.T., 1994. Cosmic ray contributions to dose rates for luminescence and ESR dating: large depth and long time variations. Radiation Measurements 23, 497–500.

Pye, K., Blott, S.J., 2004. Particle size analysis of sediments, soils and related particulate materials for forensic purposes using laser granulometry. Forensic Science International 144, 19–27.

Păunescu, Al, 2001. Paleoliticul si epipaleoliticul din spaţiul transilvan. Agir, Bucureşti.

Scheinost, A.C., 1995. Pedotransfer-Funktionen zum Wasser- und Stoffhaushalt einer Bodenlandschaft. Diss. Technische Universität München-Weihenstephan. FAM-Bericht 5, Aachen, 177 pp.

Scheinost, A.C., Schwertmann, U., 1999. Color identification of iron oxides and hydroxysulfates: use and limitations. Soil Science Society of America Journal 63, 1463–1471.

Sitlivy, V., Chabai, V., Anghelinu, M., Uthmeier, T., Kels, H., Hilgers, A., Schmidt, C., Niţă, L., Băltean, I., Veselsky, A., Hauck, T., 2012. The earliest Aurignacian in Romania: new investigations at the open air site of Românești-Dumbrăviţa I (Banat). Quartär 59, 85–130.

Sitlivy, V., Chabai, V., Anghelinu, M., Uthmeier, T., Kels, H., Niță, L., Băltean, I., Veselsky, A., Ţuţu, C. Preliminary reassessment of the Aurignacian in Banat (South-western Romania). Quaternary International (in this volume). http://dx.doi.org/10.1016/j.quaint.2012.07.024.

Soil Survey Staff, 2010. Keys to Soil Taxonomy, 11th ed. USDA-Natural Resources Conservation Service, Washington, DC. 338 p.

Szymański, W., Skiba, M., Skiba, S., 2011. Fragipan horizon degradation and bleached tongues formation in Albeluvisols of the Carpathian Foothills, Poland. Geoderma 167–168, 340–350.

Szymański, W., Skiba, M., Skiba, S., 2012. Origin of reversible cementation and brittleness of the fragipan horizon in Albeluvisols of the Carpathian Foothills, Poland. Catena 99, 66–74.

Teyssandier, N., 2003. Les débuts de l'Aurignacien en Europe. Discussion à partir des sites de Geissenklösterle, Willendorf II, Krems-Hundssteig et Bacho Kiro. Thèse de doctorat. Université de Paris X-Nanterre.

Teyssandier, N., 2007. En route vers l'Ouest. Les débuts de l'Aurignacien en Europe. In: British Archaeological Reports International Series 1638. Oxford, 312 pp.

Teyssandier, N., 2008. Revolution or evolution: the emergence of the Upper Paleolithic in Europe. World Archaeology 40 (4), 493–519.

Thiel, C., Buylaert, J.P., Murray, A., Terhorst, B., Hofer, I., Tsukamoto, S., Frechen, M., 2011. Luminescence dating of the Stratzing loess profile (Austria) – testing the potential of an elevated temperature post-IR IRSL protocol. Quaternary International 234, 23–31.

Van Vliet-Lanoë, B., 1998. Frost and soils – implications for paleosols, paleoclimates and stratigraphy. Catena 34, 157–183.

Wallinga, J., Murray, A., Wintle, A., 2000. The single-aliquot regenerative-dose (SAR) protocol applied to coarse-grain feldspar. Radiation Measurements 32 (5–6), 529–533.

Wintle, A.G., 1973. Anomalous fading of thermoluminescence in mineral samples. Nature 245, 143–144.

Wintle, A.G., Murray, A.S., 2006. A review of quartz optically stimulated luminescence characteristics and their relevance in single-aliquot regeneration dating protocols. Radiation Measurements 41, 369–391.

Witty, J.E., Knox, E.G., 1989. Identification, role in soil taxonomy and worldwide distribution of fragipans. In: Smeck, N.E., Ciolkosz, E.J. (Eds.), Fragipans: Their Occurrence, Classification, and Genesis, Soil Science Society of America Special Publication No. 24, pp. 1–9.

Zech, M., Buggle, B., Leiber, K., Marković, S., Glaser, B., Hambach, U., Huwe, B., Stevens, T., Sümegi, P., Wiesenberg, G., Zöller, L., 2009. Reconstructing Quaternary vegetation history in the Carpathian Basin, SE Europe, using n-alkane biomarkers as molecular fossils. Problems and possible solutions, potential and limitations. E&G. Quaternary Science Journal 58 (2), 148–155.

Zilhão, J., 2006. Neanderthals and Moderns mixed and it matters. Evolutionary Anthropology 15, 183–195.

Zilhão, J., Trinkaus, E., Constantin, S., Milota, Ş., Gherase, M., Sarcina, L., Danciu, A., Rougier, H., Quilès, J., Rodrigo, R., 2007. The Peştera cu Oase people, Europe's earliest modern humans. In: Mellars, P., Boyle, K., Bar-Yosef, O., Stringer, C. (Eds.), Rethinking the Human Revolution, Cambridge, pp. 249–262.

Please cite this article in press as: Kels, H., et al., Genesis of loess-like sediments and soils at the foothills of the Banat Mountains, Romania – Examples from the Paleolithic sites Româneşti and Coşava, Quaternary International (2014), http://dx.doi.org/10.1016/j.quaint.2014.04.063